Flettner rotor vessel design optimisation

Master thesis

R.J. Berendschot

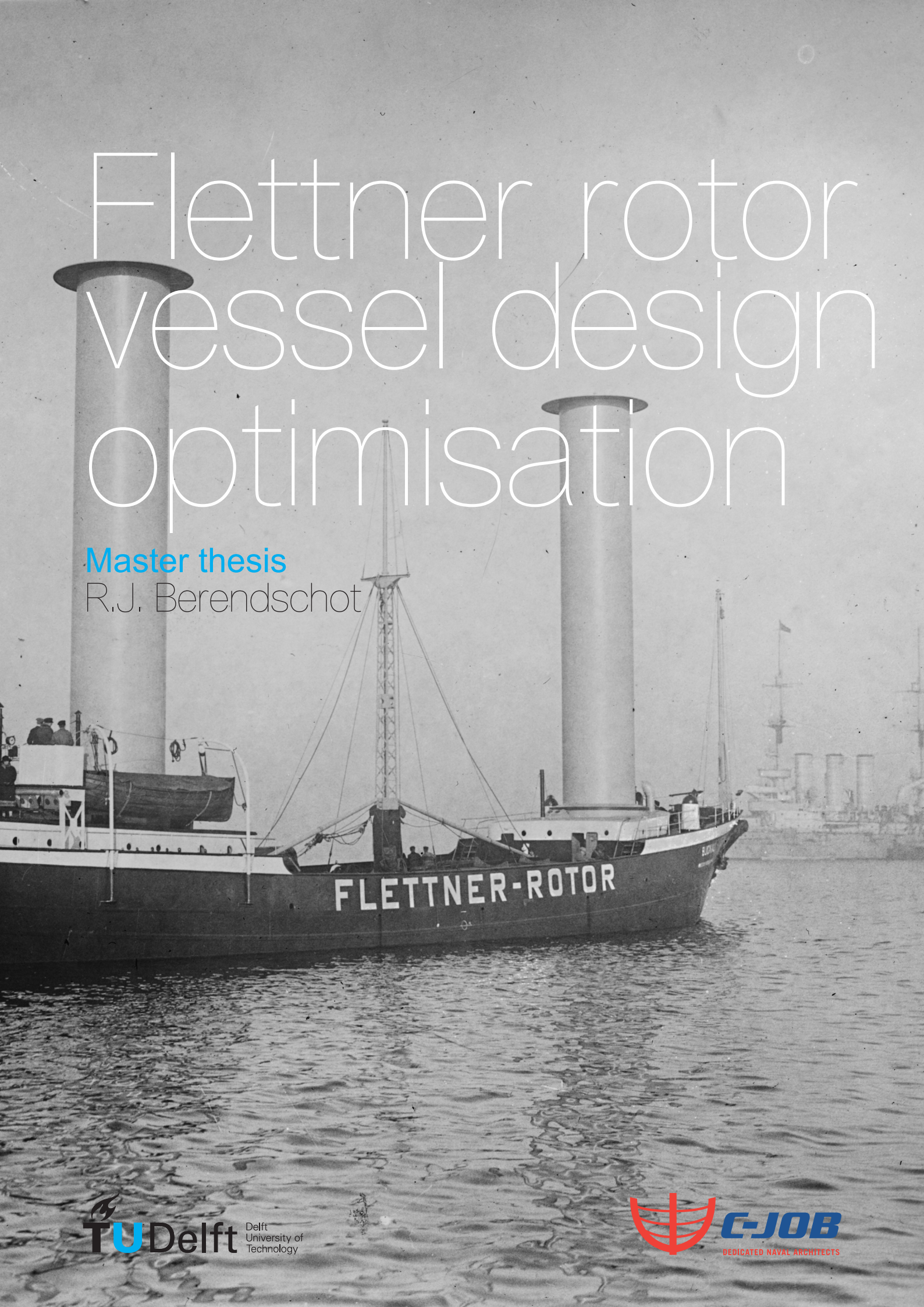

TU Delft Delft University of Technology

C-JOB DEDICATED NAVAL ARCHITECTS

Flettner rotor vessel design optimisation

Master thesis

by

R.J. Berendschot

to obtain the degree of Master of Science in Marine Technology
at the Delft University of Technology,

to be defended publicly on Tuesday September 10, 2019 at 10:00 AM.

Student number:	4221901	
Thesis company:	C-Job Naval Architechts	
Daily supervisors:	M. Dijkman MSc,	C-Job Naval Architects
	T. Muller BEng,	C-Job Naval Architects
Committee members:	Dr.ir. R.G. Hekkenberg,	TU Delft
	Dr.ir. P. de Vos,	TU Delft
	Dr. B. Atasoy,	TU Delft
	T. Vlaar BEng,	C-Job Naval Architects

An electronic version of this thesis is available at http://repository.tudelft.nl/.

Cover image from Bain News Service photograph collection

TU Delft

C-JOB DEDICATED NAVAL ARCHITECTS

Abstract

One of the most promising methods to reduce harmful emissions in shipping is to apply wind-assisted propulsion on ships. Uncertainty about the potential fuel savings makes ship owners reluctant apply wind-assisted propulsion on a large scale. The goal of this thesis is to develop a method that identifies the aspects of a vessel design, that can be optimised to minimise the payback period of Flettner rotors. In the first part of this research all cost aspects were identified that are affected by Flettner rotors. Of these cost aspects the fuel costs have the largest influence on the payback period of a Flettner rotor investment. However, these costs are also the hardest to predict in an early design stage. Therefore, this research focusses on determining the fuel savings from Flettner rotors.

To determine the fuel consumption of a ship with Flettner rotors, the Performance Prediction Program (PPP) has been developed. The PPP solves the force and moment balance equations in surge, sway, roll and yaw directions, including the physical effects from Flettner rotors. The physical phenomena that are a result of Flettner rotors lead to a number of operational characteristics whose occurrence could affect the benefits of Flettner rotors:

- To obtain heel and yaw balance, a ship with Flettner rotors is subjected to a heel angle and a rudder angle is applied. If those angles exceed operational limits, the Flettner rotors have to be throttled back, reducing their benefits.
- The side force production by the hull and rudder induces additional resistance, which has a negative contribution to the net Flettner rotor thrust.
- The thrust from Flettner rotors reduces the propeller and main engine load, changing their operating point and affecting their efficiency.

It is shown that the PPP provides accurate results, in close agreement with on-board measurements. The average savings that are predicted by the PPP differ only a few percent from the measured savings.

The Weather Routing Program (WRP) has been developed to obtain an operational profile of a ship with Flettner rotors. This operational profile is used to determine annual fuel savings, and it determines the occurrence of the operational characteristics. The WRP simulates a ship's operational conditions using historical weather data. It combines the Flettner rotor performance from the Performance Prediction Program and actual sailing schedules as input for voyage simulations. In the voyage simulations, performed by NAPA Voyage Optimization, the optimal route is calculated with the lowest fuel consumption. For some voyages the simulation data is unavailable. This leads to an underestimation of the annual fuel consumption savings from Flettner rotors and it biases the occurrence of operational characteristics.

If analysis of the WRP results shows that a operational characteristic is significantly affected by Flettner rotors, it could be considered to optimise related design aspects. A case study that was performed on a case ship with a Flettner rotor. The study demonstrates how the developed methods are used to identify aspects of a vessel design that are interesting to optimise, when Flettner rotors are applied. It was shown that the position of the Flettner rotor on the case ship has significant influence on the operational occurrence of large rudder angles and the corresponding rudder resistance. Choosing the optimal Flettner rotor location ensures adequate manoeuvring capabilities for the ship. With the Flettner rotor on its optimal position, no other measures are required to increase manoeuvring capabilities; no larger or more effective rudders are required, additional appendages do not have to be considered. The operational analysis in the case study also showed that the average engine load is significantly reduced as a result of Flettner rotors. This possibly allows to install a smaller main engine. This could reduce the Flettner rotor investment cost and decrease the Flettner rotor payback time.

Preface

With this thesis I am finishing the master's programme in Marine Technology at the Delft University of Technology. It is the completion of a seven-year long journey in Delft. In those seven years I did not only learned to build "bootjes", but I also explored Delft outside of the lecture halls. I was given the chance to take the last step of this journey at C-Job Naval Architects. Looking back, I am proud of the result that lays in front of you. Although writing this thesis is my own accomplishment, I could not have done it without the help of others.

First I want to thank Matthys Dijkman for your support and the technical discussions we had. Thank you for giving me advice, even when I did not ask for it. Thank you Thijs Muller and Geoffrey Smits for giving me guidance on moments when I was lost in my work. And I want to thank my supervisor form Delft University of Technology, Robert Hekkenberg. You helped me to find the scope of this research and gave advice on which paths to take.

I want to thank Kimmo Laaksonen, Claus Stigler and Pekka Pakkanen from NAPA and Tuomas Riski and Ville Paakkari from Norsepower. The time you spent and the data you provided is invaluable for the research I performed.

During the many months of this project, one person was always there for me. My girlfriend Emma, you kept supporting me, even when things went rough. I could always come home to you, and you would cheer me up with your smile and with your love. I cannot tell you how much you mean to me.

Finishing this project marks the end of seven amazing years in Delft. I am truly grateful for all the love and support that my parents gave me during this period. You have always encouraged me to take the beautiful opportunities that Delft had to offer me.

Robin Berendschot
Delft, September 2019

Contents

1 Introduction

This chapter gives background information to the topic of the application of Flettner rotors and wind assisted propulsion in general in section 1.1. Previous developments in this field are analysed and the relevance of this research is explained in section 1.2. In section 1.3, the goal of this research is explained and research questions are raised. Section 1.4 describes the approach of this research, and also provides the structure of this report.

1.1. Research background

Greenhouse gas emissions from the maritime industry account for approximately 3% of the total global greenhouse gas emissions [32]. Stricter environmental regulations are coming up in 2020, fuel prices are expected to increase, some estimating up to 23% [8], and the public awareness for the environment keeps growing. For these reasons vessel owners are looking for ways to save fuel consumption in the future. Applying wind-assisted propulsion is seen as a very promising solution to obtain this goal.

Wind-assisted ship propulsion is a topic of ongoing research for the past years, both at the TU Delft and at companies like C-Job Naval Architects. At the TU Delft research focuses on modelling the aerodynamic and hydromechanic implications of applying wind-assisted propulsion to vessels. At C-Job Naval Architects, concept designs have been made for vessels equipped with Flettner rotors. Here the key objective is to look at the technical implications wind-assisted ship propulsion has on a design.

In those studies, however, only rough estimations have been made for the economic benefits of wind-assisted ship propulsion. This makes vessel owners reluctant to invest in putting wind-assisted ship propulsion into practice. Giving a more complete picture of the implications of wind-assisted propulsion on a vessel could help removing this hesitation.

1.2. Research relevance

For many years now research has been done to wind-assisted ship propulsion, but the solutions have rarely been applied in practice. One of the main barriers for the implementation of wind propulsion systems is the lack of trustworthy information about the performance of those systems [26]. In the past several studies on concept vessel designs with wind-assisted propulsion have been conducted. The most recent ones include the concept design of the Ecoliner [33] using Dynarigs, the Wind Hybrid Coaster [7] and Flettner Freighter [25] both using Flettner rotors as wind propulsion. In the Ecoliner study, much emphasis has been put in to evaluate the weather routing aspects of the design [21], and also different sail configurations have been analysed. This resulted in estimated fuel savings of 28% and 14% at sailing speeds of 10kt and 12kt, respectively. In this study however, few factors are incorporated in the vessel's velocity prediction, which is suggested for further research. The same holds for the Flettner Freighter study. This study shows a possible average fuel consumption reduction of 5% to 46% at wind speeds of 10kt to 27kt, respectively. In each of the previous studies, only one concept vessel has been analysed. No methods are available to analyse an arbitrary vessel on an arbitrary route.

1.3. Objective

The goal of this research is to develop a method that determines the payback period of the capital costs involved with Flettner rotors. In a concept design stage, this method should provide an accurate prediction of the payback period for any vessel. This method should be usable to quickly analyse multiple design variations, so a designer can use the results to identify the aspects in the vessel design that can be optimised to reduce the payback period of a Flettner rotor investment. Therefore, the method should provide insight in the parameters that most influence the benefits from Flettner rotors.

From the above described research objective, the following research question rises, which will be answered in this research:

> **How can the aspects of a vessel design be identified, that can be optimised to minimise the payback period of Flettner rotors?**

Below several sub-questions have been raised to help answering the main research question. In the next section, the research approach will be explained based on these sub-questions.

What aspects of the total cost of ownership of a vessel are affected by the application of Flettner rotors?
Only aspects of a vessel design that are affected by Flettner rotors can potentially be optimised to reduce the payback period of Flettner rotors. The first step in this research is to identify those aspects.

How can the effect of Flettner rotors on the fuel consumption be quantified?
The fuel consumption is expected to be the cost aspect that has the most influence on the payback period of Flettner rotors. Determining the fuel consumption savings from Flettner rotors is not trivial, since many physical phenomena affect the performance of Flettner rotors. This research sub-question will be answered by identifying the positive and negative effects of Flettner rotors on a vessel's fuel consumption, and by providing methods to calculate these effects.

How can voyage optimisation be applied to calculate the annual fuel savings from Flettner rotors?
After answering the previous research sub-question, the fuel consumption of a vessel with Flettner rotors can be calculated in any weather condition. When the operational conditions of a vessel are known, this can be used to determine the annual fuel consumption. Even more than conventional vessels, vessels with Flettner rotors will benefit form avoiding adverse weather and pursuing beneficial weather. Using voyage optimisation algorithms, the operational conditions and fuel consumption of a vessel with Flettner rotors can be determined.

How can the influence of operational characteristics on the benefits from Flettner rotors be determined?
The operational profile of a vessel can be used to determine the occurrence of operational characteristics that influence the benefits from Flettner rotors. These operational characteristics are all physical phenomena that have influence on or are affected by Flettner rotors. Examples of these operational characteristics are additional resistance from Flettner rotors, heel angles, rudder angles and main engine loads. By analysing their operational occurrence, the operational characteristics that have a significant effect on the benefits of Flettner rotors can be identified.

1.4. Approach

The development of the above method leads to answering the research questions, using the approach as described below.

In chapter 2 all aspects of Flettner rotor application will be identified, that are likely to have a significant impact on the total cost of ownership of a vessel.

As the fuel consumption is expected to be the cost category that has the most influence on the payback period of Flettner rotors, chapter 3 discusses the development of the Performance Prediction Program (PPP). This PPP calculates the fuel consumption of a vessel with Flettner rotors in any wind condition. To calculate the fuel consumption, first the physical phenomena are identified that are caused by Flettner rotors and that affect the fuel consumption. After that, a method is proposed to quantify those physical phenomena.

Using the PPP to calculate the magnitude of the physical phenomena serves two purposes: first, it allows to calculate the fuel consumption of a vessel with Flettner rotors in any operational condition. The second purpose is that it allows for comparing the relative importance of different physical phenomena that are a result of Flettner rotors. A naval architect can potentially optimise a vessel design to reduce negative effects of certain physical phenomena, or increase the positive effects of other phenomena.

Which aspects of a vessel design are interesting to optimise depends on the occurrence of the corresponding physical phenomena. This occurrence is determined by a vessel's operational profile. Therefore, these phenomena will be referred to as *operational characteristics* in this report.

In chapter 4 the Weather Routing Program (WRP) is discussed. The WRP uses results from the PPP and a vessel's sailing schedule to perform voyage optimisation analyses. This results in annual fuel savings from Flettner rotors. A second result from the WRP is an overview of the influence of operational characteristics on the benefits of Flettner rotors. This overview helps identifying the aspects of a vessel design that can be optimised to minimise the payback period of Flettner rotors.

In chapter 5 a case study is performed, that demonstrates how the developed methods are used to identify aspects of a case vessel design that are interesting to optimise, when Flettner rotors are applied on the case ship.

Finally in chapter 6, conclusions of this research are drawn and recommendations for future research are made.

2

Cost categories affected by Flettner rotors

For a vessel owner, the decision to install one or more Flettner rotors on a vessel is based on the trade-off between the costs and benefits of the Flettner rotor(s). In this chapter the financial aspects of this trade-off are identified.

The capital investment costs associated with Flettner rotors are discussed in section 2.1. Reductions in operating and voyage costs determine the feasibility to invest in installing Flettner rotors. Section 2.2 identifies which aspects of operating and voyage costs are likely to be affected significantly by Flettner rotors.

2.1. Capital investment costs

When investing in installing Flettner rotors, there are both direct and indirect costs to take into account. Direct investment costs are the purchase of the rotors, installation costs and costs for the rotor foundation. Indirect investment costs are costs involved with optimising other parts of the vessel, with the aim of increasing the benefits from the Flettner rotors.

2.1.1. Direct investment costs

Direct investment costs associated to Flettner rotors are independent of the type of vessel where they are installed on. The height of these costs mainly depends on the number and size of Flettner rotors that is installed. The costs of Flettner rotors typically ranges from $\$\,400\,000$ for smaller rotors, to $\$\,950\,000$ for larger rotors [9]. The foundation and the installation of the rotors is included in this price.

2.1.2. Indirect investment costs

When alterations to a vessel design are made to increase the benefits from the Flettner rotors, the costs for these alterations should be considered as indirect investment costs. Examples of such design optimisations could include changes to the hull shape, additional appendages and main engine selection. Which of those changes in the vessel design are potentially interesting is very case-specific. This depends on the occurrence of corresponding operational characteristics, as will be discussed in chapter 4.

Besides costs associated with the above mentioned design optimisations, another indirect investment cost category exists. Installing Flettner rotors and their foundations increases the lightship weight of a vessel, decreasing its deadweight and cargo carrying capacity. In this research it is assumed that installing Flettner rotors should not affect the earning capacity. To prevent a loss in earning capacity of the vessel, the vessel size needs to increase to compensate for the deadweight that is decreased by the Flettner rotors.

2.2. Affected operating costs and voyage costs

The effects of installing Flettner rotors on operating costs and voyage costs determine the return on investment and payback period of the Flettner rotor investment. A breakdown of the major cost categories of a vessel is shown in figure 2.1. This section discusses the effect of installing Flettner rotors on each of the components of the operating costs and voyage costs, and what method can be used to quantify this effect.

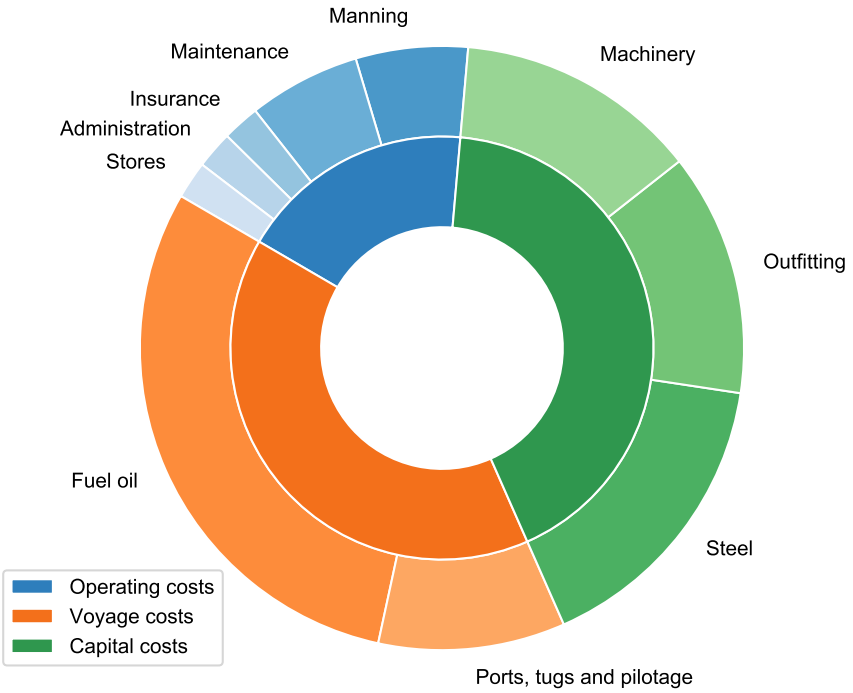

Figure 2.1: Breakdown of vessel cost categories, adopted from Stopford [34, pp. 225, 544]

- Operating costs
  - Manning: The influence on the manning costs is limited, since computer-controlled Flettner rotor systems are commercially available. The crew only requires a short training and operating the system does not increase the workload of the crew [37].
  - Maintenance: The Flettner rotor systems require additional maintenance costs. Flettner rotor suppliers provide this maintenance as a service, for an fixed annual fee as a function of the size and number of rotors.
  - Insurance: Class approved Flettner rotors are available, ensuring that rotors are capable of safely operating in all operational and environmental situations [3]. Therefore insurance costs are not expected to be affected by Flettner rotors.
  - Administration and stores: These cost categories are not expected to be affected by Flettner rotors.
- Voyage costs
  - Fuel oil: Unlike the manning and maintenance costs, the effect on fuel oil costs is not simply a fixed amount. The effect of Flettner rotors on the fuel oils costs depends on many factors like vessel dimensions, sailing speed, operating profile and weather conditions. It is not possible to accurately quantify the fuel consumption savings without information about all these factors. Since this is the largest cost category of a vessel that is affected by Flettner rotors, a method to estimate this effect is required.
  - Ports, tugs and pilotage: When rotors are placed in suitable locations, discharge times are not affected. Tugs costs could affected slightly, because rotors increase the vessel's wind

profile, affecting the manoeuvrability. The available research the effect of rotors on manoeuvrability while berthing and unberthing is limited. Although this introduces a factor of uncertainty to this cost category, this cost category is comparatively small and the effect is expected to be limited. Therefore this effect will not be taken into account in this study.

2.3. Conclusion

Three different types of investment costs are identified associated with Flettner rotors: direct costs of the Flettner rotors, costs associated with vessel design optimisations to increase the rotor benefits, and costs associated with the compensation for the vessel's deadweight that is reduced by installing the rotors.

Fuel costs is the main cost category affected by Flettner rotors that determines the payback period of the rotor investment costs. Since the effect of cost category is hard to estimate, a model will be developed which can be used to predict the fuel savings from Flettner rotors. This model is described in the following chapters.

3

Performance Prediction Program

In the previous chapter it was identified that the fuel consumption is the cost category that has the most influence on the payback period of a Flettner rotor investment, and it is also the hardest cost category to estimate in an early design stage.

This chapter describes the Performance Prediction Program (PPP), the model that is developed to determine the magnitude of all physical phenomena that are a result of Flettner rotors. This is used to calculate fuel consumption of any vessel in any operating condition. In the next chapter, this relationship between operating conditions and fuel consumption is used to determine the annual fuel savings from Flettner rotors.

The core of this PPP is to find an equilibrium in all forces and moments at play when Flettner rotors are installed. Section 3.1 introduces the physical phenomena that occur when Flettner rotors are operating on a vessel. This results in an overview of the forces and moments that need to be balanced to obtain equilibrium in the surge, sway, roll and yaw directions.

All these physical phenomena have an effect on the benefits from Flettner rotors. In a concept design stage, the magnitude of a number these physical phenomena can be influenced. This way, the benefits of Flettner rotors can be influenced. The effects of these physical phenomena will be referred to as *operational characteristics*, since their occurrence depends on a vessel's operational profile. Section 3.2 provides an overview of the operational characteristics that are affected by Flettner rotors. For each operational characteristic potential solutions are proposed that a naval architect could apply to increase the benefits from Flettner rotors. Chapter 4 will elaborate on the method that is used to determine which of the operational characteristics are interesting for vessel optimisation.

In section 3.3 an overview is given of typical values for orders of magnitude of the forces, moments and other operational characteristics that are an effect of the application of Flettner rotors. After that, the rest of this chapter discusses the calculation method of each of these Flettner rotor effects.

First, the calculation of rotor forces is presented in section 3.4. The heel balance is explained in section 3.5. The hull side force and the rudder forces that influence the side force and yaw balance are explained in sections 3.6 and 3.7. In section 3.8 those forces and their associated resistance are used to calculate the total resistance. In section 3.9 this total resistance, combined with the thrust from the rotors, is used to calculate the required propeller thrust and engine load. This also determines the fuel consumption. When all components of the force and moment balance equations are accounted for, section 3.10 provides a method to solve them. To validate this method, the results of the performance prediction program are compared to onboard measurements in section 3.11.

To conclude this chapter, in section 3.12 the range in which the PPP is applicable is summarised, together with corresponding recommendations for further research.

3.1. Force balance

The forces at play that need to be balanced by the PPP are shown in figure 3.1. The methods that are implemented to calculate each of these forces are explained in the following sections.

The force balance in x-direction is shown in equation (3.1). Flettner rotors generate a part of the forward thrust required to propel the ship: X_{FR}. To balance the total ship resistance, the other part of the thrust needs to be delivered by the propeller: $T_{P,E}$. The total ship resistance consists of the calm water resistance R_{CW}, wave added resistance R_{WA} and induced hull and rudder resistance ($R_{H,i}$ and X_R, respectively). These last two resistance components are a direct result of Flettner rotors.

As a consequence of Flettner rotor side force Y_{FR}, the vessel obtains a drift angle ψ. This introduces a side force on the hull Y_H and on the rudder Y_R. The hull and rudder side force balance the rotor side force, see equation (3.2). The side force production of the hull and rudder also induces additional resistance $R_{H,i}$ and X_R in equation (3.1).

The longitudinal location of the aerodynamic and hydrodynamic side forces generally do not coincide, so yaw moments are introduced: $M_{z,H}$, $M_{z,R}$ and $M_{z,FR}$ for the hull, rudder and Flettner rotors, respectively. A rudder angle δ is required to balance the yaw moments, see equation (3.3).

The side force of the rotors also introduces a heeling moment $M_{x,FR}$. The result is a heel angle ϕ at which the hydrostatic righting moment $M_{x,H}$ is equal and opposite to the heeling moment: equation (3.4).

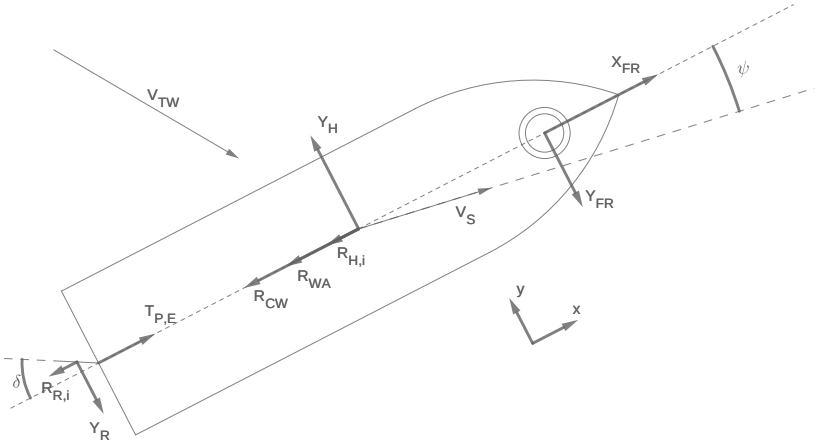

Figure 3.1: Flettner rotor force, angle and velocity overview.

$$T_{P,E} + X_{FR} + R_{CW} + R_{WA} + R_{H,i} + R_{R,i} = 0 \tag{3.1}$$

$$Y_{FR} + Y_H + Y_R = 0 \tag{3.2}$$

$$M_{z,FR} + M_{z,H} + M_{z,R} = 0 \tag{3.3}$$

$$M_{x,FR} + M_{x,H} = 0 \tag{3.4}$$

3.2. Operational characteristics

The operational characteristics that are influenced by Flettner rotors, or have an influence on the benefits of Flettner rotors are discussed below. If an operational characteristic is significantly affected by Flettner rotors, a naval architect should consider to optimise related aspects of a vessel design. In chapter 4 will be discussed how the occurrence of the operational characteristics can be determined. For each operational characteristic, potential design solutions are provided that could increase the benefits from Flettner rotors.

The affected operational characteristics are grouped in four categories. First, the heel and rudder equilibrium angles are discussed in subsection 3.2.1. Second, additional resistance components as a

result of Flettner rotors is discussed in subsection 3.2.2. Third, Flettner rotors lead to changes in the required propeller thrust. As a result the operational point of the propeller and the main engine changes, of which the effects are discussed in subsection 3.2.3. Also potential changes in sailing speed are discussed. Fourth and last, the forces, rotation speed and power consumption of the Flettner rotors are discussed in subsection 3.2.4.

3.2.1. Equilibrium angles

To obtain heel moment equilibrium, a vessel with Flettner rotors is subjected to a heel angle; for yaw moment equilibrium a rudder angle has to be applied. Large heel or rudder angles could affect the benefits form Flettner rotors.

Heel angle

In certain operational conditions, large heel angles can occur as a result of the Flettner rotor side forces and resulting heeling moments. When these heel angles exceed certain comfort or safety limits, the Flettner rotors are throttled back to reduce the rotor side forces. This also reduces the forward thrust from the rotors, and thus leads to lower fuel savings.

When the rotor thrust has to be reduced in a significant part of a vessel's operational profile to keep heel angles acceptable, the vessel designer might consider to change the vessel design. A first possible solution is to reduce the heeling arm by moving the Flettner rotors to a lower location, while taking into account that the rotors should keep operating in undisturbed airflow. A second solution is to increase the vessel stability, for example by increasing the vessel breadth or length, or by lowering the centre of gravity.

Rudder angle

When large rudder angles are required to counteract Flettner rotor yaw moments, they could compromise the vessel's manoeuvrability. In those operational conditions, the Flettner rotors are throttled back, reducing their yaw moments. However, this also reduces the fuel saving benefits from the rotors.

When this reduction of rotor benefits is significant in a vessel's operational profile, the vessel designer could apply the following solutions to reduce the required rudder angles:

- The most straightforward solution is to move the rotors towards the centre of lateral pressure of the hull, which reduces the yaw moment arm of the rotors. As will be explained in section 3.6, this centre of pressure generally lays near the front of the vessel. Depending on the application, moving all rotors forward is not always feasible.
- Another way to reduce the yaw moment arm is to move the centre of lateral pressure more aft. This could be obtained by changing the hull shape or by applying additional appendages to the hull, like skegs [17] or bilge keels [36].
- A last possible solution to reduce the required rudder angles is to increase the capability of rudders to generate side force. This can either be done by applying more effective rudder shapes, or by installing more or larger rudders.

3.2.2. Additional resistance

The generation of side force by the hull and rudder induces additional resistance. This resistance reduces the net Flettner rotor propulsive force. When this reduction of net propulsive force leads to a significant decrease in annual fuel savings, measures could be considered to reduce the induced resistance components.

Induced hull resistance

Possible reductions for the hull induced resistance could be obtained by increasing the efficiency of hull side force production. Model tests have showed that bilge keels improve can the hull side force efficiency [36].

Induced rudder resistance

The most straightforward solution to reduce induced rudder resistance is to reduce the required rudder angles, for which solutions are suggested in section 3.2.1. Also the induced rudder resistance could

be reduced by increasing the rudder efficiency (side force to resistance ratio). Recommendations for efficient rudder design are for example given by Liu and Hekkenberg [15].

3.2.3. Propulsion efficiency

For any vessel, the required propeller thrust and engine load depends on the weather conditions the vessel is sailing in. For a vessel with Flettner rotors, the nature of this dependency changes. On average, the required propeller thrust and engine load decreases, but also the variation in propeller thrust and engine load increases with changing operating conditions.

Propeller efficiency

When the operational analysis shows that the required propeller thrust is significantly affected by Flettner rotors, the propeller could be optimised for delivering a lower average thrust or a larger thrust variation. For example, installing controllable pitch propellers instead of fixed pitch propellers could increase the overall propulsion efficiency.

Engine load

Similar to the propeller, the average engine load is expected to reduce and to be more variable as a result of Flettner rotors. This could affect the engine's specific fuel consumption. Possibly the propulsion efficiency could be increased by a lower installed main engine power or by alternative engine configurations, for example a diesel-electric configuration.

Sailing speed

A consequence of applying Flettner rotors in combination with voyage optimisation is that a vessel deviates from its normal (shortest) route to pursue favourable weather conditions. As a result, the average sailing speed could increase, while still the fuel consumption is reduced. This means that the vessel's hull could be optimised for this higher average sailing speed, or for a larger range of speeds.

3.2.4. Flettner rotor characteristics

The last group of operational characteristics are related to the Flettner rotors themselves. As will be explained in section 3.4, Flettner rotors are subjected to a number of operational limitations. Analysis of the operational profile can reveal that the Flettner rotors operate at their limits. These limits could concern the maximum allowable forces on the rotor, the maximum rotational speed or the maximum power of their motors. If the rotors operate at their limits often, it could be considered to install rotors higher capacities, even though they are more expensive. This information could also be useful for the Flettner rotor suppliers, since it provides more insight in the actual operating conditions.

3.3. Typical values of Flettner rotor effects

To illustrate the relative importance of the forces, moments and other operational characteristics at play, two different Flettner rotor configurations are analysed on the Ro-Ro cargo ship M/V Estraden. The first configuration has one small Flettner rotor, the second configuration has two larger rotors.

3.3.1. Rotor configurations

In November 2014, a Norspower Rotor Sail, with a height of $18\,\mathrm{m}$ and diameter of $3\,\mathrm{m}$ was installed on the aft of the M/V Estraden. A year later, a second rotor was installed amidships, see figure 3.2. From the first test period, with one rotor installed, Norsepower has shared measurement data which is used to verify the results of the Performance Prediction Program (PPP). This verification is explained in section 3.11.

Typical conditions from this test period are used to illustrate the magnitude of the different effects of Flettner rotors that are modelled in the PPP. Two Flettner rotor configurations have been modelled to demonstrate these effects. The first configuration has one small rotor installed on the aft of the vessel, as it was applied on the M/V Estraden. Also, to show the effect of installing more and larger rotors, a second rotor configuration, with two larger $30\,\mathrm{m}$ by $5\,\mathrm{m}$ Flettner rotors, has been analysed by the PPP. This configuration of the rotors is the same as installed on the M/V Estraden, but the rotor size has been increased. Particulars of the M/V Estraden and the rotor configurations are shown in table 3.1.

Figure 3.2: Two Norsepower Rotor Sails installed on the M/V Estraden [22].

Table 3.1: Analysed configurations of Flettner rotors on the M/V Estraden.

M/V Estraden vessel data			
Length over all		162.7	m
Breadth		25.7	m
Draught		6.6	m
DWT		9 700	ton
Propulsion power		14 480	kW
Design service speed		19	kt
Rotor configurations	**1 18x3m rotor**	**2 30x5m rotors**	
(x, y, z) from (APP, CL, BL)	(0, 7, 10)	(0, 7, 10), (50, 7, 10)	m
Rotor height	18	30	m
Rotor diameter	3	5	m

3.3.2. Typical conditions

Relatively strong wind conditions are used to illustrate the effects of Flettner rotors. The force and moment balances from equations (3.1) to (3.4) were solved for a true wind speed of $8\,\mathrm{m\,s^{-1}}$ (4 Bft), a true wind direction of $90°$ and a ship speed of $15\,\mathrm{kt}$. It should be noted that this ship speed the most common sailing speed in the trial period, but it is significantly lower than the design service speed. In table 3.2, the balanced forces and moments in these conditions are shown, together with the relevant angles and powers for which these are balanced.

Equilibrium angles

Solving the force equilibrium from equations (3.1) to (3.4) in the described typical conditions leads to yaw, rudder and heel angles that are shown in table 3.2. In both rotor configurations, the yaw angles are very small. As will be further explained in section 3.6, these yaw angles lie well within the range of yaw angles for which the Performance Prediction Program provides accurate results.

Similar to the yaw angles, the calculated heel angles are small, justifying the assumption of small heel angles in the heel angle calculation as explained in section 3.5.

The typical rudder angle in the configuration with one small rotor is small ($1.0°$), agreeing with experiences of the crew that the rotor had no recognizable effect on the rudder angles [37]. In the configuration

Table 3.2: Angles, forces and power for two Flettner rotor configurations on the M/V Estraden, sailing at 15kt in 8 m s^{-1} (4 Bft) beam wind. *Values hidden for confidentiality reasons.*

Angles [°]		**1 small rotor**	**2 large rotors**
Yaw angle	ψ	–	–
Rudder angle	δ_R	–	–
Heel angle	ϕ	–	–
X-force balance [kN]			
Effective propeller thrust	$T_{P,E}$	–	–
Rotor thrust	X_{FR}	–	–
Calm water resistance	R_{CW}	–	–
Wave added resistance	R_{WA}	–	–
Hull induced resistance	$R_{H,i}$	–	–
Rudder induced resistance	$R_{R,i}$	–	–
Y-force balance [kN]			
Rotor side force	Y_{FR}	–	–
Hull side force	Y_H	–	–
Rudder side force	Y_R	–	–
Yaw balance [kN m]			
Rotor yaw moment	$M_{z,FR}$	–	–
Hull yaw moment	$M_{z,H}$	–	–
Rudder yaw moment	$M_{z,R}$	–	–
Power [kW]			
Main engine brake power	P_B	–	–
Brake power savings	$P_{B,savings}$	–	–
Rotor rotation power	P_{FR}	–	–
Fuel consumption [kg h^{-1}]			
Main engine fuel consumption	$\dot{m}_{ME}$	–	–
Flettner rotor fuel consumption	$\dot{m}_{FR}$	–	–
Total fuel consumption	$\dot{m}_{tot}$	–	–
Fuel consumption savings	$\dot{m}_{savings}$	–	–

with two large rotors, the calculated typical rudder angle is 5.2°. Rudder angles of this magnitude do not significantly impair the manoeuvring capabilities of a ship. It does suggest however that larger, and thus rudder angles could occur in more extreme operational conditions. This requires for a calculation method that is able to accurately estimating the forces involved with large rudder angles, which will be explained in section 3.7.

X-force balance

Table 3.2 shows that the Flettner rotor provides 3 % of the total required thrust. In the configuration with two large rotors the rotors deliver 18 % of the required thrust. The hull and rudder induced resistance have only a slight negative influence on the net rotor thrust. In both rotor configurations, the induced hull resistance is less than 1 % of the rotor thrust. The induced rudder resistance less than 2 %.

The calculation method of the hull and rudder induced resistance components is explained in sections 3.6 and 3.7, respectively. Small errors are introduced in these calculations, but since the additional resistance components are relatively small, these errors have a negligible effect on the x-force balance.

Y-force balance

In the described typical situations, the rotor side forces are approximately twice as large as the rotor thrust forces. The resulting opposite hydrodynamic side forces are generated by the hull and the rudder. The relative contribution of the hull to the total hydrodynamic side force is relatively larger for the

configuration with two large rotors compared to the configuration with one small rotor. This is a direct result from the fact that the second rotor in the two-rotor configuration is positioned more forward on the ship.

Yaw balance

The yaw moments shown in table 3.2 correspond to the side forces from the Flettner rotors, hull and rudder. The relation The yaw moments in table 3.2 are obtained by multiplying the side forces with their corresponding yaw moment arms. The moment arm for the Flettner rotor side force is determined by their location and the rotation torque, as explained in section 3.4. The method for determining the hull and rudder yaw moments is explained in sections 3.6 and 3.7, respectively.

Power and fuel consumption

Some values in this section are hidden for confidentiality reasons. The typical main engine brake power and fuel consumption is shown in table 3.2, as calculated by the PPP using the method that is described in section 3.9. The power and fuel consumption savings are obtained by comparing these numbers with the PPP results for the same ship without Flettner rotors. Without Flettner rotors, the main engine brake power equals $6\,400$ kW at the specified sailing speed of 15 kt. This is in correspondence to the $14\,480$ kW of installed engine power for the 19 kt design speed.

The brake power savings that are a result of the Flettner rotors are – % for the configuration with one small Flettner rotor and – % for the configuration with two large rotors. The power required for rotating the Flettner rotors is – % of the main engine brake power savings for both rotor configurations.

The main engine fuel consumption savings are similar to the brake power savings. The total fuel consumption savings are $-\,\mathrm{kg\,h^{-1}}$ and $-\,\mathrm{kg\,h^{-1}}$ for the configurations with one small rotor and two large rotors, respectively. These are relative savings of 3 % and 17 %.

3.4. Rotor forces and power consumption

Flettner rotors use the Magnus effect to generate a lift force that contributes to the propulsion of a ship, as illustrated in figure 3.3. The lift and drag forces generated by the rotor and the power consumed by the rotor determine the fuel savings from the main propulsion system. The lift force, drag force and rotation power are given by, respectively:

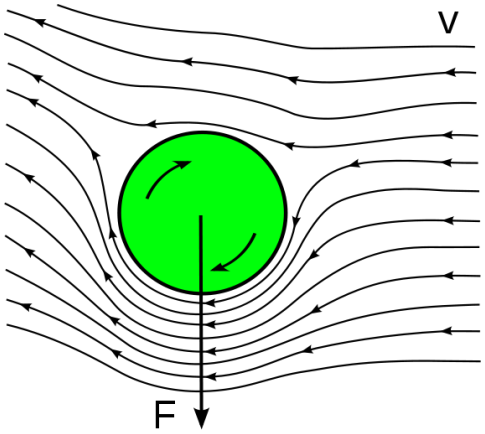

Figure 3.3: Illustration of the Magnus effect.

$$L_{FR} = C_L \cdot \frac{1}{2} \cdot \rho \cdot V_{AW}^2 \cdot A \cdot \cos\phi \tag{3.5}$$

$$D_{FR} = C_D \cdot \frac{1}{2} \cdot \rho \cdot V_{AW}^2 \cdot A \tag{3.6}$$

$$P_{FR} = C_P \cdot \frac{1}{2} \cdot \rho \cdot V_{AW}^3 \cdot A \tag{3.7}$$

where C_L, C_D and C_P are the lift, drag and power coefficients, respectively, V_{AW} is the apparent wind velocity as defined in figure 3.4, A is the projected area of the rotor; the product of its diameter and height. Lastly, α is the spin ratio; the ratio between the apparent wind velocity and the circumferential velocity of the rotor surface, which is given by

$$\alpha = \frac{n \cdot \pi \cdot d}{V_{AW}} \tag{3.8}$$

where n is the rotation rate of the rotor and d is the rotor diameter.

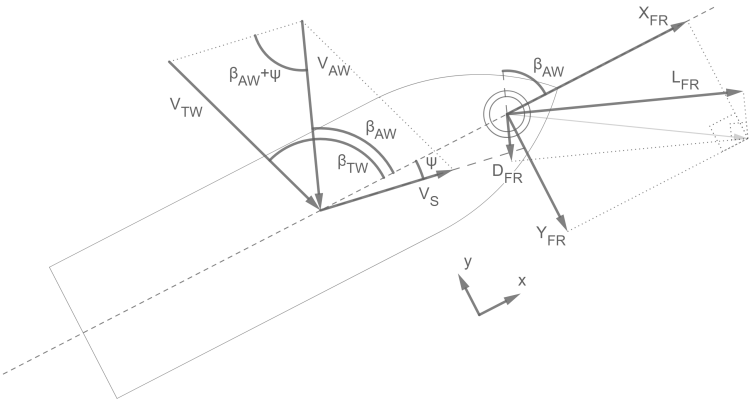

Figure 3.4: Wind angle and rotor force definition.

3.4.1. Rotor parameters

Research has shown that several parameters have influence on the aerodynamic performance of Flettner rotors, such as the Reynolds number Re, aspect ratio and endplate configurations. The best choice of these parameters will be discussed below.

Reynolds number

The range of Reynolds numbers (equation (3.9), where ν is the kinematic viscosity) that is of interest in this study can be estimated by looking at existing Flettner rotor applications. Reynolds numbers approximately range from 10^5 for small rotors ($d = 3\,\mathrm{m}$) in low apparent wind speeds of $0.5\,\mathrm{m\,s^{-1}}$, to 10^7 for large rotors ($d = 6\,\mathrm{m}$) in high apparent wind speeds of $30\,\mathrm{m\,s^{-1}}$.

$$Re = \frac{V_{AW} \cdot d}{\nu} \tag{3.9}$$

Aspect ratio

Similar to sails, rotors with higher aspect ratios deliver more thrust per unit surface area [6, 30]. Therefore high aspect ratio rotors are desired. The rotor height and diameter are limited by practical reasons such as air draught, structural strength and space occupation. This trade-off resulted in aspect ratios of around 6 in most commercial applications [37] and experiments [1]. The rotor aspect ratio in this study will therefore be fixed at 6.

Endplate configurations

Adding endplates to rotating cylinders reduces pressure losses at the ends of the rotor, similar to the effect of wingtips at conventional wings. Larger endplates result in higher aerodynamic efficiencies, but also increases the power required to rotate the rotor. According to experiments by Badalamenti and Prince [1], the best trade-off between aerodynamic efficiency and required power lays at a endplate diameter ratio $d_e/d = 1.5 - 2.0$, where d_e is the diameter of the endplate. This is the range of diameter ratios that will be used in this study.

Lift and drag coefficient

Experimental and numerical studies show good agreement for values of the lift and drag coefficients as a function of spin ratio [1, 6, 27, 35]. The results also show that the lift and drag coefficients are not affected by the Reynolds number, and therefore a fixed relationship exists between the lift and drag ratios and the spin ratio of a rotor. In this study, the results from Badalamenti and Prince [1] for rotors with aspect ratio of 6 and endplate diameter of $d_e/d = 2$ will be used. The lift and drag coefficients are shown in figure 3.5. Norsepower Oy Ltd. has equipped multiple vessels with their Flettner rotors. Their measurement data closely resemble the presented lift and drag coefficients. Due to confidentially reasons, this measurement data cannot be shared in this report.

These lift and drag coefficients are used in equations (3.5) and (3.6). In these equations it is assumed that the rotors operate in undisturbed airflow. In practice, the incoming airflow can be disturbed when rotors are placed in proximity of cargo on deck, superstructures and other rotors. These effects are not taken into account in this study. To prevent significant errors in the rotor force calculations, rotors should be placed at a sufficient distance from objects obstructing the incoming airflow. Norsepower advises this distance to be greater than the height of the rotors.

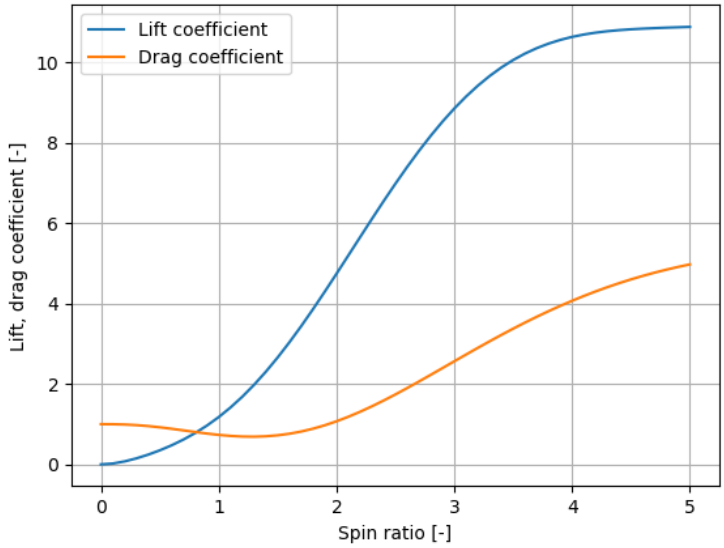

Figure 3.5: Lift and drag coefficient as a function of spin ratio [1].

Rotation power

The power that is required to rotate a Fettner rotor is determined by the flow speed at the rotor's surface. In a potential flow, the flow past a rotating two-dimensional cylinder can be described as the superposition of a vortex flow and the flow around a non-rotating cylinder. With this, the local flow speed at every point on the cylinder can be calculated, allowing to calculate the local skin friction. Integrating this friction along the total rotor surface gives the torque required to rotate the rotor. This derivation can be found in Masset [16], Norwood [24]. The resulting power coefficient C_P, as used in equation (3.7), is given by:

$$C_P = C_f \cdot \pi \cdot (2 + \alpha^2) \cdot \alpha \tag{3.10}$$

In here C_f is the friction coefficient as calculated by the Prandtl-Schlichting formula. At low spin ratios, the flow speed around the rotor is dominated by the apparent wind speed, so the Reynolds number Re from equation (3.9) is used to calculate C_f. At higher spin ratios, the flow speed is dominated by the rotor rotation speed. In this case the rotational Reynolds number $Re_\phi = \frac{1}{2} \cdot Re \cdot \alpha$ is used to calculate C_f:

$$C_f = \frac{0.472}{(\log_{10} \max(Re, Re_\phi))^{2.58}} \tag{3.11}$$

The same method is used to determine the power required to rotate the rotor's endplates. To validate this method as used in the PPP, the results are compared with experiments from Bordogna et al. [4], as can bee seen in figure 3.6. The used calculation method assumes potential flow, ignoring any viscous effects like flow separation. Despite this simplification, the calculated rotation power closely match the observed values. The power prediction lays within the range of different measurements.

The presented method was also compared with measurements on rotors installed on several vessels by Norsepower Oy Ltd. The calculated power consumption largely falls within the range of Norsepower's measurement variation. Only for the higher spin ratios ($\alpha > 4$) the power consumption is over-predicted. Due to confidentially reasons, this measurement data cannot be shared in this report.

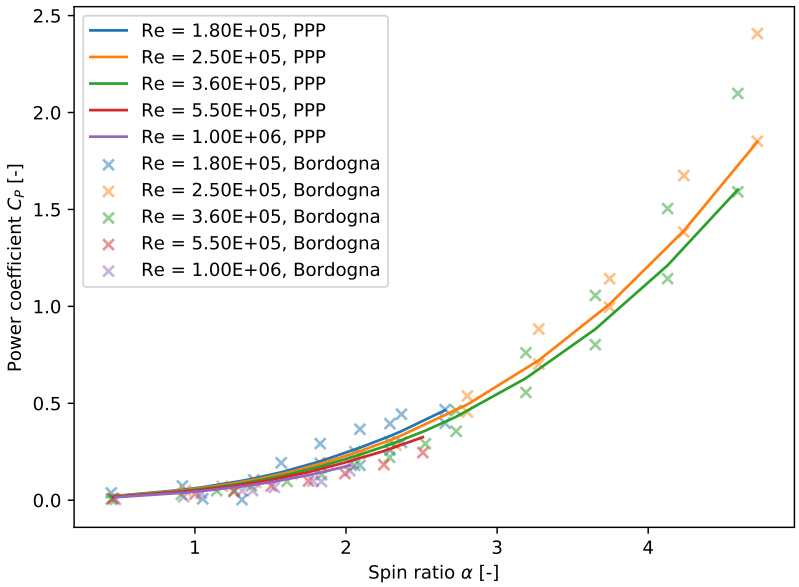

Figure 3.6: Dimensionless rotor power C_P, as defined in equation (3.10), as a function of spin ratio α. PPP-calculations compared with experiments from Bordogna et al. [4].

3.4.2. Thrust and side force

To calculate the contributions of the lift and drag forces of the rotor to the ship propulsion, the forces are projected to the ship's x- and y-axes (see figure 3.4). The thrust of the Flettner rotor in x-direction is defined as

$$X_{FR} = L_{FR} \cdot \cos\phi \cdot |\cos(\beta_{AW} + \pi/2)| + D_{FR} \cdot \cos(\beta_{AW} + \pi) \tag{3.12}$$

where the lift force always has a component in the positive x-direction, since the direction of rotor rotation is set to deliver forward thrust. When under heel, only the horizontal lift component is taken into account. The drag force, by definition, only has a horizontal component since it is parallel to the wind.

Similarly, the side force is the sum of the lift and drag projected on the y-axis:

$$Y_{FR} = L_{FR} \cdot \cos\phi \cdot \sin(\beta_{AW} + \pi/2) + D_{FR} \cdot \sin(\beta_{AW} \pm \pi) \tag{3.13}$$

where the direction of the y-component of the drag force is opposite to the apparent wind direction (see figure 3.4).

3.4.3. Operating limitations

Three factors limit the rotation speed of Flettner rotors: the driving motor maximum rotation speed, the motor power and the loads on the bearings. The values of these practical limits as used in this study are taken from Norsepower Oy Ltd. [23]. A rotor with a height of 30 m and diameter of 5 m for example, can rotate up to 180 rpm, using at most 110 kW. The maximum total force on the rotor is 270 kN. An example of rotor thrust and side forces generated by this rotor is shown in figures 3.7 and 3.8.

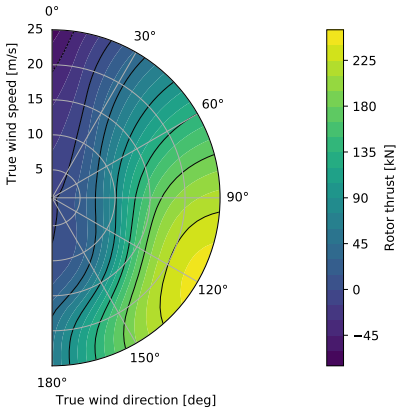

Figure 3.7: Thrust force from a 30 m by 5 m Flettner rotor on a vessel sailing at 15 kt

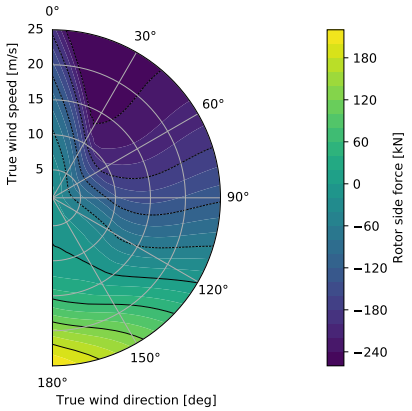

Figure 3.8: Side force from a 30 m by 5 m Flettner rotor on a vessel sailing at 15 kt

3.5. Heel balance

The heeling moment $M_{x,FR}$ from equation (3.4) is the product of the heeling rotor side force Y_{FR} and the heeling arm z_{Mx}; the vertical distance from the centre of the Flettner rotor to the centre of the underwater lateral area which is approximated at a point at half the vessel draught. The righting lever l_r that is required to counteract the heeling force from the Flettner rotors is calculated with

$$l_r = \frac{Y_{FR} \cdot z_{Mx}}{\rho \cdot g \cdot \nabla} \tag{3.14}$$

Assuming small heel angles, the heel angle ϕ can be calculated with

$$\phi = \arcsin\left(\frac{l_r}{GM}\right) \tag{3.15}$$

where GM is the metacentric height. When the metacentric height is not known for the analysed vessel, it can be estimated, for example by using the method from Schneekluth and Bertram [29].

Typical values for heel angles do not exceed 1°, as shown in table 3.2. This validates the assumption of small heel angles in equation (3.15).

When, in extreme wind conditions, heel angles exceed a threshold value, the rotor spin ratio is reduced in the PPP. This results in a lower rotor side force, reducing the heel angle. The heel angle threshold value can be specified by the user of the PPP.

3.6. Hull side force

To predict the hydrodynamic forces acting on the hull as a result of a leeway angle, a regression model proposed by Kang and Hasegawa [12] is used. This parametric model predicts hydrodynamic side force, induced resistance and yaw moment at the entire operating speed range of a vessel, while many other prediction methods only look at forces when manoeuvring at low speeds.

Model description

The regression model from Kang and Hasegawa [12] determines the non-dimensional forces and moment coefficients as used in the following equations:

$$R_{H,i} = R'_{H,i} \cdot \frac{1}{2} \cdot \rho \cdot V_S^2 \cdot L_{pp} \cdot T \tag{3.16}$$

$$Y_H = Y'_H \cdot \frac{1}{2} \cdot \rho \cdot V_S^2 \cdot L_{pp} \cdot T \tag{3.17}$$

$$M_{z,H} = M'_{z,H} \cdot \frac{1}{2} \cdot \rho \cdot V_S^2 \cdot L_{pp}^2 \cdot T \tag{3.18}$$

where $R_{H,i}$ is the induced resistance of the hull due to leeway, Y_H is the generated side force, and $M_{z,H}$ is the yaw moment. $R'_{H,i}$ and Y'_H are the induced resistance coefficient and side force coefficient. $M_{z,H}$ is the yaw moment coefficient. The parameters on which the regression model is based are the ship's main dimensions; length, breadth, draught and block coefficient. Next to these main parameters, also two stern hull parameters are used in the model: the prismatic coefficient of the aft hull C_{pa} and the water plane area coefficient of the aft hull C_{wa}, which are used to calculate the fullness parameters e'_a and σ_a [14].

$$X'_H = \left(a_{x1} \cdot \sin^2(\psi) + a_{x2} \cdot \sin^2(2\psi)\right) \cdot \cos(\psi) \tag{3.19}$$

$$Y'_H = a_{y1} \cdot \sin(\psi) + a_{y2} \cdot \sin(3\psi) + a_{y3} \cdot \sin(5\psi) \tag{3.20}$$

$$M'_{z,H} = a_{m1} \cdot \sin(2\psi) + a_{m2} \cdot \sin(4\psi) \tag{3.21}$$

$$a_{x1} = \frac{B}{L_{pp}} \cdot \left(-0.54867 + 11.791 \cdot \frac{T}{L_{pp}}\right) \tag{3.22a}$$

$$a_{x2} = 2 \cdot \frac{T}{L_{pp}} \left(-0.07237 - 0.52608 \cdot \frac{B}{L_{pp}}\right) \tag{3.22b}$$

$$a_{y1} = 0.50194 + 5.3541 \cdot \frac{T}{L_{pp}} \tag{3.22c}$$

$$a_{y2} = -0.08788 + 0.73174 \cdot \frac{C_b B}{L_{pp}} \cdot K \tag{3.22d}$$

$$a_{y3} = -0.10285 + 1.9317 \cdot \frac{T\,(1 - C_b)}{B} \cdot K \tag{3.22e}$$

$$a_{m1} = \frac{B}{L_{pp}} \cdot \left(0.07093 + 1.1936 \cdot \frac{T}{B}\right) \tag{3.22f}$$

$$a_{m2} = K \cdot \left(-0.052545 + 0.42428 \cdot \frac{C_b B}{L_{pp}} K\right) \tag{3.22g}$$

$$\sigma_a = \frac{1 - C_{wa}}{1 - C_{pa}} \tag{3.23a}$$

$$e'_a = \frac{\left(1 - C_{pa}\right) L/B}{\sqrt{\frac{1}{4} + \frac{1}{(B/d)^2}}} \tag{3.23b}$$

$$K = \left(\frac{1}{e'_a} + \frac{1.5}{L/B} - 0.33\right) \cdot (0.95\sigma_a + 0.40) \tag{3.23c}$$

Verification and validation

The implementation of Kangs model in the PPP is verified by comparing calculated side force coefficients with experiments as reported by Kang and Hasegawa [12], see figures 3.9 and 3.10. Calculated values show a very good match with experimental data, especially for small yaw angles. As shown in table 3.2, yaw angles as a result of Flettner rotor side forces generally do not exceed $1°$. The induced resistance as a result of these yaw angles is very small, not exceeding 0.5 % of the rotor thrust in almost all conditions.

The range of ship parameters that is used in Kangs regression model, is shown in table 3.3. When ships with parameters outside this range are used, the results should be treated with care. However, since yaw angles and the resulting resistance generally is very small, this is not expected to have a significant effect on the results of the PPP.

As mentioned in section 3.5, heel angles are expected to be very small. Therefore, heel angles are not taken into account when calculating the hull side force. Several studies have indicated heel angles do influence the side force production of a hull [5, 11], so if the PPP were to be used in scenarios with larger heel angles, further research into this influence is required.

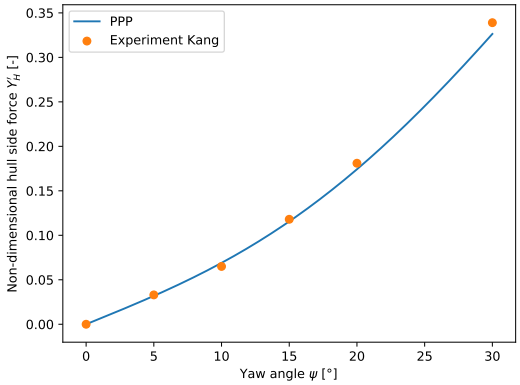

Figure 3.9: Side force due to leeway; PPP calculations compared with experiments as reported by Kang and Hasegawa [12]

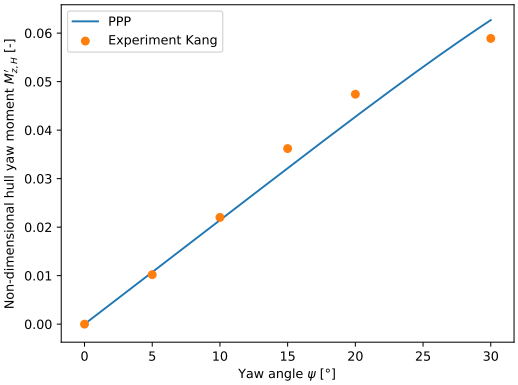

Figure 3.10: Hull yaw moment due to leeway; PPP calculations compared with experiments as reported by Kang and Hasegawa [12]

Table 3.3: Applicable ship parameter ranges used in the regression model of Kang and Hasegawa [12]

Ship parameter	Min	Max
B/L	0.163	0.2
T/L	0.055	0.073
T/B	0.302	0.411
C_b	0.777	0.833

3.7. Rudder forces

For the calculation of forces generated by the rudder, the mathematical model of Kijima et al. [14] is used. This model is based on the same mathematical model as used for calculating the hull forces due to leeway in section 3.6. The implementation of this model in the PPP is discussed in this section. First an overview is given of the different rudder forces at play. After that, the rudder lift and drag coefficients are discussed, followed by different interaction effects: flow straightening, rudder wake and rudder-on-hull interactions. Lastly this method will be verified.

Rudder force overview

The forces of interest acting on the rudder are shown in figure 3.11.

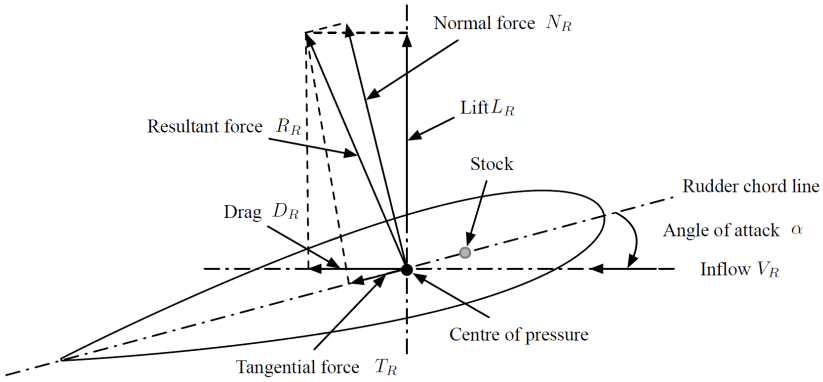

Figure 3.11: Forces acting on a rudder, copied from Liu and Hekkenberg [15].

To calculate the rudder forces in the ship forward direction X_R and sideways direction Y_R, the corresponding yaw moment M_R, and the rudder induced resistance $R_{R,i}$,the following equations are used:

$$X_R = C_{X,R}\frac{1}{2}\rho V_R^2 A_R \tag{3.24}$$

$$Y_R = C_{Y,R}\frac{1}{2}\rho V_R^2 A_R \tag{3.25}$$

$$M_R = C_{M,R}\frac{1}{2}\rho V_R^2 A_R L_{PP} \tag{3.26}$$

$$R_{R,i} = X_R - X_{R0} \tag{3.27}$$

$$C_{X,R} = -(1-t_R)(C_{N,R}\sin\delta - C_{T,R}\cos\delta) \tag{3.28}$$

$$C_{Y,R} = -(1+a_H)(C_{N,R}\cos\delta + C_{T,R}\sin\delta) \tag{3.29}$$

$$C_{M,R} = -(x'_R + a_H x'_H)(C_{N,R}\cos\delta + C_{T,R}\sin\delta) \tag{3.30}$$

$$C_{N,R} = C_{L,R}\cos\alpha_R + C_{D,R}\sin\alpha_R \tag{3.31}$$

$$C_{T,R} = -C_{L,R}\sin\alpha_R + C_{D,R}\cos\alpha_R \tag{3.32}$$

where $C_{X,R}$, $C_{Y,R}$ and $C_{M,R}$ are the non-dimensional force and moment coefficients in surge, sway and yaw direction, respectively. X_{R0} is the rudder resistance in neutral position without yaw. V_R is the rudder inflow velocity and A_R is the rudder area. $C_{N,R}$ and $C_{T,R}$ are the normal and tangential force coefficients (see figure 3.11). $C_{L,R}$ and $C_{D,R}$ are the lift and drag force coefficients. Rudder-hull interaction coefficients t_R, a_H, x_R and x_H will be discussed below. Lastly, α_R is the rudder angle of attack and δ the rudder angle relative to the ship centreline. Their relationship is governed by flow straightening, which will be discussed below.

Rudder lift and drag coefficient

As mentioned by Liu and Hekkenberg [15], in the method of Kijima et al. [14] only the normal rudder force N_R is taken into account to calculate the resulting forces and moments in surge, sway and yaw direction. The tangential rudder force T_R is neglected. Since the purpose of the PPP is to calculate the fuel consumption of a vessel, forces in surge direction are of great importance, so the tangential forces cannot be neglected in the current application. Therefore the normal rudder force is not calculated directly using Kijima's method, but instead the lift and drag coefficients are used, see equations (3.31) and (3.32).

The factors that influence the lift and drag coefficients of a rudder are extensively discussed by Molland and Turnock [19], whose empirical formulas will be used here. The lift coefficient is calculated using:

$$C_{L,R} = \left[\frac{\mathrm{d}C_{L,R}}{\mathrm{d}\alpha_R}\right]_{\alpha_R=0} \cdot \alpha_R + \frac{C_{Dc,R}}{K_R}\alpha_R^2 \tag{3.33}$$

$$\left[\frac{\mathrm{d}C_{L,R}}{\mathrm{d}\alpha_R}\right]_{\alpha_R=0} = \frac{1.95\pi}{1+\frac{3}{K_R}} \tag{3.34}$$

$$C_{Dc,R} = 0.1 + 1.6\frac{c_{T,R}}{c_{R,R}} \quad \text{Square tips} \tag{3.35}$$

$$C_{Dc,R} = 0.1 + 0.7\frac{c_{T,R}}{c_{R,R}} \quad \text{Faired tips} \tag{3.36}$$

where $c_{T,R}/c_{R,R}$ is the taper ratio of the rudder; the ratio between the tip and the root chord length. K_R is the effective aspect ratio. This is the most influential parameter when determining the lift and drag coefficient and is given by:

$$K_R = k\frac{h_R}{c_R} \tag{3.37}$$

$$k = 2 - 0.016\left|\frac{180}{\pi}\delta\right| \tag{3.38}$$

where h_R is the rudder height and c_R the average chord length. The hull acts as a reflection plane for the rudder, significantly increasing the effective aspect ratio of the rudder, compared to the geometric aspect ratio. This influence decreases with increasing rudder angles, as calculated by the effective aspect ratio factor k.

The drag coefficient is calculated using the drag at angle of attack of zero $C_{D0,R}$ and the induced drag factor k_i:

$$C_{D,R} = C_{D0,R} + k_i\frac{C_{L,R}^2}{K_R} \tag{3.39}$$

Based on other published data, Molland and Turnock [19] suggest a value for $k_i = 0.37$. $C_{D0,R}$ is a function of the thickness to chord ratio t_R/c_R. Its value is in the range of $C_{D0,R} = 0.009 - 0.012$ for $t_R/c_R = 0.05 - 0.22$, respectively [19, Fig 5.19].

Flow straightening

When a vessel has a drift angle ψ, the rudder angle of attack α_R is affected, as shown in figure 3.12. The flow straightening effect from the propeller reduces the effect of drift on the angle of attack. The relationship between the angle of attack α_R and the angle relative to the ship centreline δ is calculated using the flow straightening factor γ_R.

$$\alpha_R = \delta - \gamma_R \cdot \psi \tag{3.40}$$

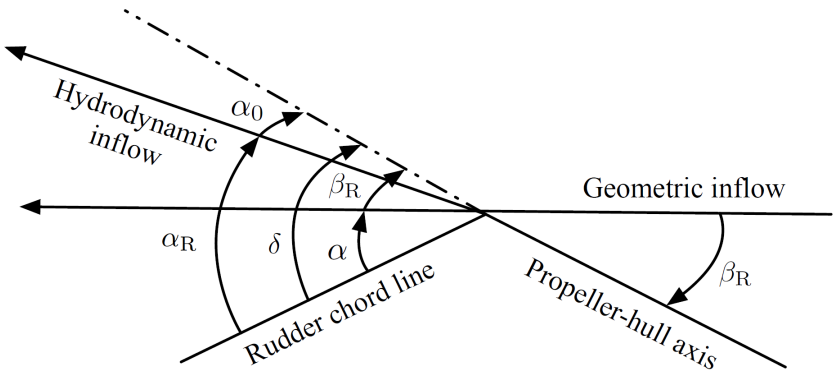

Figure 3.12: Flow straightening, copied from Liu and Hekkenberg [15]

The flow straightening factor depends on the shape of the (aft) hull. Kijima et al. [14] proposed approximate formulae to predict γ_R, using the aft hull shape fullness parameter e'_a from equation (3.23):

$$\gamma_R = 4.0197\frac{T\,(1-C_b)}{B} + 1.9776\left\{\frac{T\,(1-C_b)}{B}e'_a\right\}^2 - 1.5442\left\{\frac{T\,(1-C_b)}{B}e'_a\right\} + 0.218 \tag{3.41}$$

Rudder wake

The flow velocity around the hull decreases around the aft ship, and is increased again by the propeller. The resulting inflow speed of the rudder V_R is determined by the rudder wake fraction w_R:

$$V_R = (1-w_R)V_S\sqrt{1+g(s)} \tag{3.42}$$

where $g(s)$ is a function to incorporate the effects of the thrust loading from the propeller, given by the following equation:

$$g(s) = \eta K\{2-(2-K)s\}s/(1-s)^2 \tag{3.43}$$

$$\eta = \frac{D_P}{h_R} \tag{3.44}$$

$$K = 0.6\,\frac{(1-w_P)}{(1-w_R)} \tag{3.45}$$

$$s = 1-(1-w_P)\,\frac{V_S\cos\psi}{n_P P_P} \tag{3.46}$$

The rudder wake fraction coefficient w_R can be calculated using:

$$w_R = w_{R0}\frac{w_P}{w_{P0}} \tag{3.47}$$

$$w_{R0E} = -7.4406\frac{TC_b}{L} - 2.3907\frac{C_bB}{L}\sigma_a + 0.851 \tag{3.48}$$

$$w_P = w_{P0}\exp\left(-4.0\psi^2\right) \tag{3.49}$$

where w_{R0} and w_{P0} are the wake fraction coefficients in straight forward moving at the rudder and propeller, respectively. σ_a is an aft ship section fullness parameter from equation (3.23) [14].

Rudder-on-hull interaction

As explained by Simonsen [31], a rudder action behind a hull results in an increase in lateral force on the hull. This effect is captured by the factor a_H in equation (3.29). The yaw moment arm corresponding to this lateral force is captured by non-dimensional distance between the centre of gravity of ship and centre of additional lateral force x'_H in equation (3.30). The last rudder-on-hull interaction effect at play is the thrust deduction. The propeller accelerates the flow around the hull, resulting in additional resistance, which is captured in the propeller thrust deduction coefficient. The resistance from the rudder slows down the flow around the aft ship, resulting in the opposite effect. This is captured in the rudder thrust deduction coefficient $(1-t_R)$ in equation (3.28). Empirical relationships are proposed by Kijima et al. [13] to calculate a_H, x'_H and $(1-t_R)$ using C_b:

$$(1-t_R) = 0.28\,C_b + 0.55 \tag{3.50}$$

$$a_H = 2.0571\,C_b^2 - 0.5205\,C_b - 0.1052 \tag{3.51}$$

$$x'_H = 8.75\,C_b^2 - 7.0018\,C_B - 0.3847 \tag{3.52}$$

Verification

First, the determination of lift and drag coefficients will be verified (equations (3.33) to (3.39)), since this part of calculating the rudder forces deviates from Kijima's proposed method. Experimental results from Whicker and Fehlner [38] will be used for the lift and drag coefficient verification. In figures 3.13 and 3.14 the experimental results are shown for a NACA0015 rudder, with geometric aspect ratio $K_{R,G} = 1.5$, taper ratio $c_{T,R}/c_{R,R} = 0.45$ and square tips, performed at a Reynolds number $Re = 2.70\cdot10^6$. It can be seen that the calculated coefficients almost exactly match the experiments.

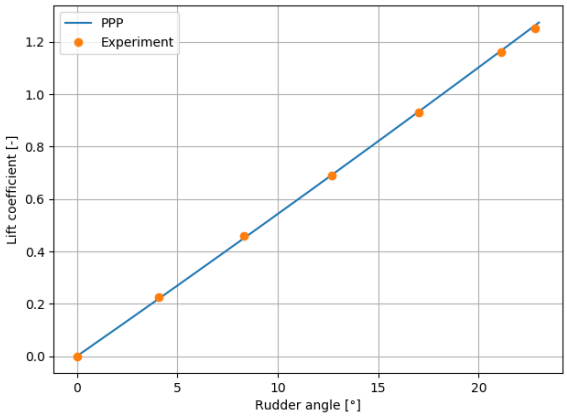

Figure 3.13: Lift coefficient for a NACA0015 rudder in free stream. Experimental results from Whicker and Fehlner [38]

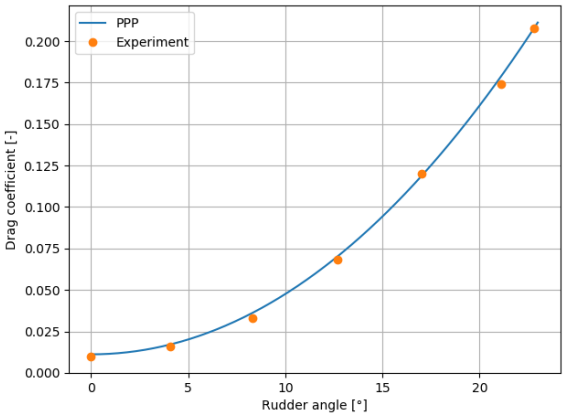

Figure 3.14: Drag coefficient for a NACA0015 rudder in free stream. Experimental results from Whicker and Fehlner [38]

The rudder forces in the wake of a hull and propeller (equations (3.40) to (3.52)), with various drift angles are verified using experiments from Molland and Turnock [18]. The verification case is a NACA0020 rudder behind a 'Mariner' hull [28] and a Wageningen B-Series propeller. In figure 3.15 can be seen that the lift coefficients calculated by the PPP lie within 5 % of the experimental values for small drift angles. For larger drift angles however, the differences increase to around 15 % at larger rudder angles.

Generally, rudder and drift angles are small ($5°$ and $1°$, table 3.2), so the rudder lift forces are calculated appropriately. In more extreme wind conditions, when also large rotors are placed in less suitable locations on the ship, calculated required rudder angles to keep a straight course could increase to larger values of $25°$ to $30°$. The aforementioned 15 % uncertainty in the lift coefficient calculation leads to an overestimation of the required rudder angles.

To prevent inaccurate rudder angle calculations, the user of the PPP could specify a rudder angle threshold value. When larger rudder angles occur, the Flettner rotor spin ratio is reduced by the PPP, reducing the rotor yaw moments that need to be compensated by the rudder. This however, also reduces the rotor thrust, and consequently the fuel savings.

The error between predicted and measured drag coefficients ranges from 30 % to 45 % at high rudder and drift angles, see figure 3.16. The prediction method from Kijima et al. [13], without taking rudder tangential forces into account, gives errors up to 70 %. In the typical range of rudder and drag angles (table 3.2), the error in the drag coefficient reaches 10 %. In these conditions, the magnitude of the rudder resistance is less than 1 % of the thrust that is delivered by the Flettner rotors. Therefore, a 10 % error in the rudder resistance calculation will have no significant influence on the fuel savings from the Flettner rotors.

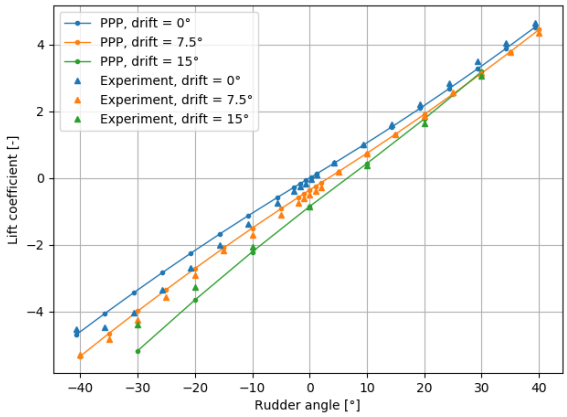

Figure 3.15: Lift coefficient for a NACA0020 rudder behind a 'Mariner' hull. Experimental results from Molland and Turnock [18]

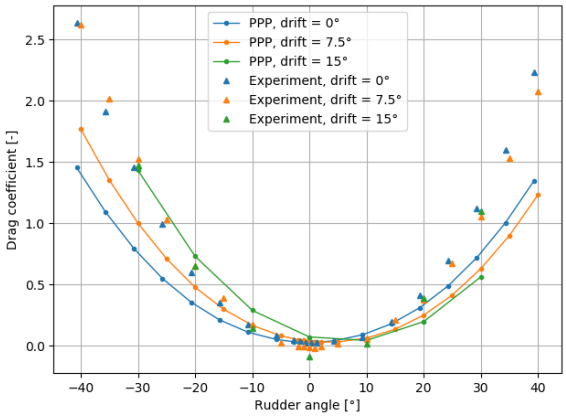

Figure 3.16: Drag coefficient for a NACA0020 rudder behind a 'Mariner' hull. Experimental results from Molland and Turnock [18]

3.8. Resistance

The total resistance as used in equation (3.1) consists of the calm water resistance R_{CW}, added resistance in waves R_{WA}, induced resistance due to hull side force $R_{H,i}$ and the rudder induced resistance $R_{R,i}$:

$$T_{P,E} + X_{FR} + R_{CW} + R_{WA} + R_{H,i} + R_{R,i} = 0 \qquad \text{(ref. (3.1))}$$

Of these resistance components, $R_{H,i}$ and $R_{R,i}$ have already been discussed in sections 3.6 and 3.7, respectively. The calm water resistance and added resistance in waves will be discussed in the following subsections.

3.8.1. Calm water resistance

A widely used method for the prediction of calm water resistance, is the method from Holtrop and Mennen [10]. NAPA, a Finnish maritime software, services and data analysis provider, has concluded that often the actual resistance deviates from the predictions by Holtrop and Mennen (personal communication). Therefore NAPA devolved its own resistance prediction model based on measured performance data on a wide range of cargo vessels. This resulted in a validated database of speed-resistance curves for any existing cargo ship (within the scope of NAPA). This speed-resistance curve database forms the basis of the calm water resistance prediction in the PPP. The speed-resistance curve for the M/V Estraden, used for validating the PPP, is shown in figure 3.17.

When the PPP is used for performance prediction of an existing ship, the speed-resistance curve from NAPA's database is used. In the case that design variations of such an existing vessel have to be evaluated, the speed-resistance curves can be manually adjusted using other prediction methods like Holtrop and Mennen.

3.8.2. Added resistance in waves

Similar to the calm water resistance, NAPA has estimated the added resistance in waves for many existing vessels. The wave added resistance coefficient c_{RWA} estimation is available as a function of ship speed V_S, wave angle of attack β_{wave} and wave zero crossing period T_0. The wave added resistance R_{WA} is calculated using the following equation, where H_S is the significant wave height:

$$R_{WA} = c_{WAR}(V_S, \beta_{wave}, T_0) \cdot H_S^2 \qquad (3.53)$$

Since the Performance Prediction Program calculates the fuel consumption based on the wind conditions, a direct relationship between wind and wave conditions is implemented. A fully developed sea is assumed, so the Pierson-Moskowitz wave spectrum can be applied [20]. The significant wave height and zero crossing period are calculated according to Pierson-Moscowitz is calculated using:

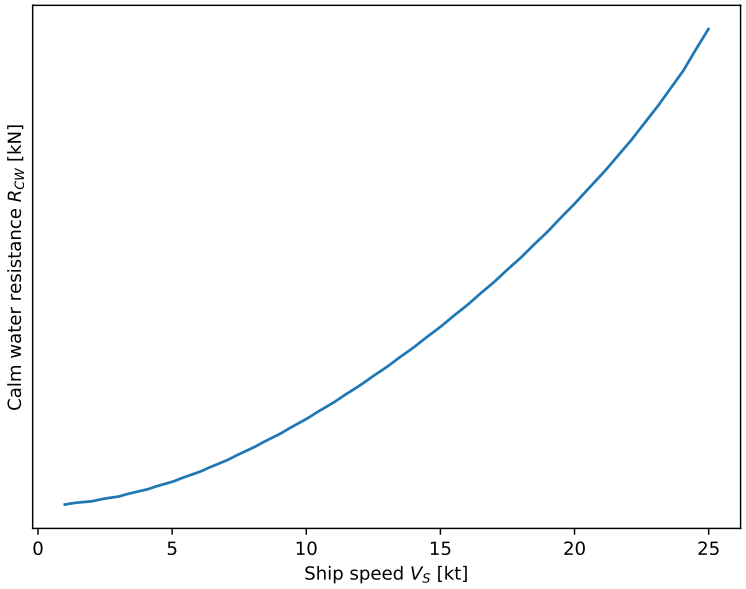

Figure 3.17: Resistance of the M/V Estraden, as provided in the NAPA Performance model. *Axis values hidden for confidentiality reasons.*

$$H_S = 0.22\frac{V_{TW}^2}{g} \tag{3.54}$$

$$\omega_p = 0.877\frac{g}{V_{TW}/1.026} \tag{3.55}$$

$$T_0 = 0.711\frac{2\pi}{\omega_p} \tag{3.56}$$

where V_{TW} is the wind speed at 10 m above sea level and ω_p is the wave peak frequency. The incoming wave direction is assumed to be equal to the incoming wind direction.

For vessel designs that are not in NAPA's reference database, a similar vessel from the database can be used. Alternatively, wave added resistance coefficients can be provided manually, for example calculated using a panel method.

3.9. Fuel consumption

In sections 3.4 and 3.8 the Flettner rotor thrust force X_R and total ship resistance R_{tot} have been discussed, respectively. Together these determine the effective propulsive thrust that is required from the propeller $T_{P,E}$, see equation (3.1). To calculate the fuel consumption of the vessel, this section discusses the total power chain efficiency: first the propulsive efficiency, followed by the transmission and engine efficiency.

3.9.1. Propulsive efficiency

Three factors make up the total propulsive efficiency η_D: the hull efficiency η_H, open water efficiency η_H and relative rotative efficiency η_R.

Hull efficiency

For many existing ships NAPA provides the thrust deduction coefficient t_P and propeller wake fraction in straight forward moving condition w_{P0}. The influence of drift angles and flow straightening on the wake fraction has been discussed in section 3.7, see equation (3.49). The propeller thrust T_P, advance velocity V_A, thrust power P_T and hull efficiency η_H are calculated using:

$$T_P = \frac{R_{tot}}{1 - t_P} \tag{3.57}$$

$$V_A = (1 - w_P)V_S \tag{3.58}$$

$$P_T = T_P V_A \tag{3.59}$$

$$\eta_H = \frac{1 - t_P}{1 - w_P} \tag{3.60}$$

Open water efficiency

For many existing ships NAPA provides the thrust and torque coefficients in their performance models, allows to determine the propeller open water efficiency. Figure 3.18 shows the thrust and torque coefficients and open water efficiency for the M/V Estraden as provided by NAPA. When no performance model is available, the Wageningen B-Series open water diagrams [2] are used to determine the open water efficiency of a propeller (fixed pitch). When only the propeller diameter d_P and the number of blades are known, the optimal blade area ratio is estimated using the method from Holtrop and Mennen [10] at the ship design speed. This is then used to find the optimal propeller pitch P using the Wageningen B-series data. With these propeller dimensions known, the open water propeller curves of the are given by the B-series polynomials. These curves, together with the required thrust T_P and advance velocity V_A, are used to obtain the propeller torque Q_P, open water efficiency η_O and rotation speed n_P.

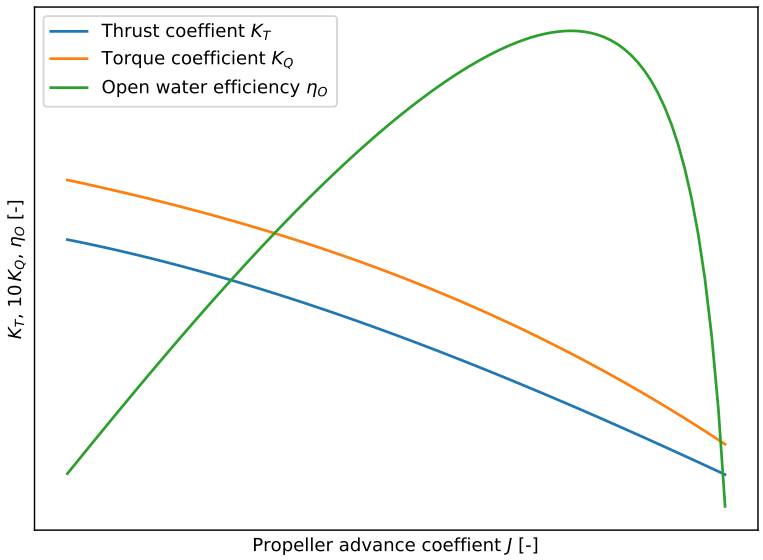

Figure 3.18: Thrust and torque coefficients and open water efficiency of the M/V Estraden, as provided in the NAPA Performance model. *Axis values hidden for confidentiality reasons.*

Power delivered to propeller

Together with the relative rotative efficiency η_R, provided by NAPA, the open water efficiency and hull efficiency are used to calculate the total propulsive efficiency η_D, which relates the effective thrust power P_E to the power delivered to the propeller P_P:

$$P_P = \frac{P_E}{\eta_D} = \frac{P_E}{\eta_O \cdot \eta_R \cdot \eta_H} \tag{3.61}$$

3.9.2. Transmission and engine efficiency

The transmission efficiency (shafting efficiency η_S and gearbox efficiency η_{GB} if applicable) is provided for existing vessels by NAPA, which is used to calculate the main engine brake power P_B. Also the

specific fuel consumption SFC_{ME} is given by NAPA, as function of the engine load. The specific fuel consumption of the M/V Estraden is shown in figure 3.19. This is used to calculate the main engine fuel consumption $\dot{m}_{f,ME}$:

$$P_B = \frac{P_P}{\eta_S \cdot \eta_{GB}} \tag{3.62}$$

$$\dot{m}_{f,ME} = P_B \cdot SFC_{ME} \tag{3.63}$$

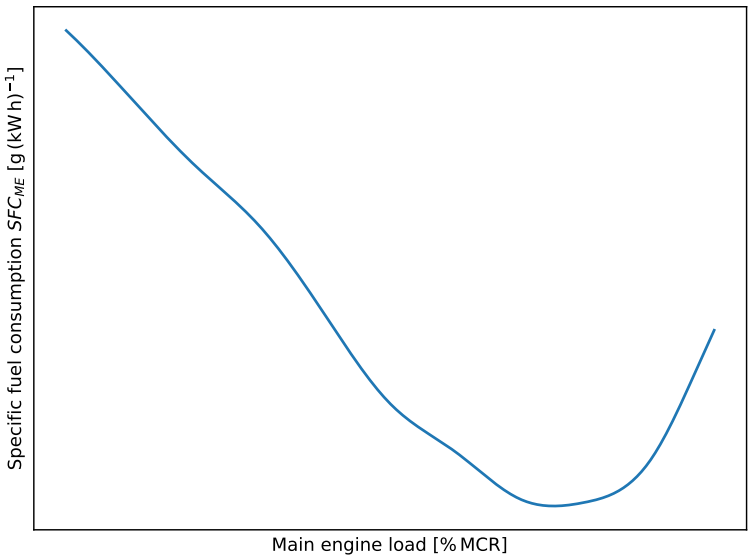

Figure 3.19: Main engine specific fuel consumption of the M/V Estraden, as provided in the NAPA Performance model. *Axis values hidden for confidentiality reasons.*

3.9.3. Flettner rotor fuel consumption

In section 3.4 the power that is required to rotate a Flettner rotor has been determined. To include losses in the electric motor and rotor bearings, a Flettner rotor efficiency factor η_{FR} is introduced, for which a value of 0.9 is assumed. Currently, it is assumed that the electrical power is generated using auxiliary engines with an specific fuel consumption SFC_{aux} of 200 g (kW h)$^{-1}$. The fuel consumption for rotating a Flettner rotor, $\dot{m}_{f,FR}$, therefore becomes:

$$\dot{m}_{f,FR} = \frac{P_{FR}}{\eta_{FR}} \cdot SFC_{aux} \tag{3.64}$$

3.9.4. Fuel savings

The total fuel consumption $\dot{m}_{tot}$ of a vessel with Flettner rotors is determined by adding the main engine fuel consumption and the Flettner rotor fuel consumption, see equation 3.65. To calculate the fuel savings $\dot{m}_{savings}$ that are obtained by the Flettner rotors, the PPP is used to analyse the same vessel without Flettner rotors, and the results are compared.

$$\dot{m}_{tot} = \dot{m}_{f,ME} + \dot{m}_{f,FR} \tag{3.65}$$

3.10. PPP solving method

To obtain force equilibrium in x- and y-direction and moment equilibrium about the x- and z-axis, the calculation method of the performance prediction model is shown in figure 3.20. The rotor forces depend on the rotor spin ratio α. The spin ratio value that results in the lowest fuel consumption is determined

in the PPP, for each combination of ship speed, wind speed and wind angle that has to be analysed. Below the structure of this method is explained in more detail.

1. Specify a combination of ship speed, wind speed V_{TW} and true wind angle β_{TW} for which the performance has to be calculated. Like in prediction programs for conventional sailing vessels this is the first step of the PPP. Additionally, specify the ship speed V_S. This allows for solving the required propeller thrust, which is not necessary in pure sailing vessel prediction programs.
2. Select an initial value for the rotation rate α. The rotation rate of a Flettner rotor determines the forces it generates. With given wind conditions and vessel speed, different rotation rates result in different rotor forces and thus different fuel consumption. This means that, for each wind condition, an optimal rotation rate exists that results in minimum fuel consumption of the vessel. The optimal rotation rate is therefore determined iteratively.
3. Choose first values for the heel angle ϕ and leeway angle ψ.
4. Calculate the Flettner rotor lift, drag and required rotation power. Calculate the heeling moment from the FR side force.
5. Using the specified value for heel angle ϕ, calculate the righting moment.
6. Compare the heeling and righting moments. When unequal, change the heel angle and repeat steps 4 and 5. If the maximum allowable heel angle is exceeded, the FR side force is to high and α has to be reduced.
7. Using the specified value for leeway angle ψ, calculate the hydrodynamic side force that is produced by the hull and the resulting resistance. Calculate the longitudinal location of the centre of effort of the side force.
8. Calculate the yaw moments delivered by the Flettner rotors and the hull side force. Calculate the rudder angle required to counteract those moments and the resulting resistance.
9. Compare the aerodynamic and hydrodynamic side force. When unequal, change the leeway angle and repeat steps 4 to 9.
10. Calculate the calm water resistance, resistance due to heel and added resistance in waves. Add the resistance due to side force and rudder angle. Subtract the thrust delivered by the Flettner rotors. The remaining resistance determines the thrust that the propeller must deliver. Using the propulsion efficiency, calculate the fuel consumption. Calculate the fuel consumption to rotate the Flettner rotors.
11. When all values of rotation rate α are evaluated, the rotation rate that results in the lowest total fuel consumption is the optimal rotation rate for this combination of V_{TW}, β_{TW} and V_S.
12. For the optimal rotation rate, store the fuel consumption, rotor forces and other relevant parameters. Proceed to the next combination of wind conditions and ship speed until all combinations are analysed.

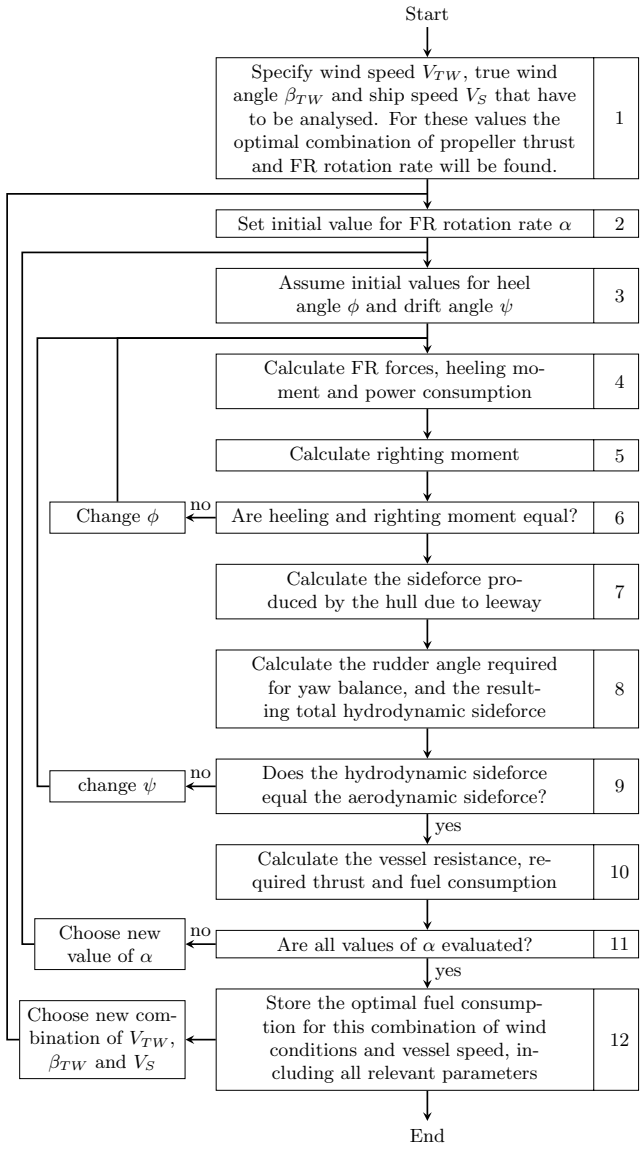

Figure 3.20: Schematic PPP calculation method

3.11. PPP validation

Using on-board measurements, NAPA has calculated the power savings attained by a Norsepower rotor sail on board of the Ro-Ro cargo ship Estraden. During an eight-month period, the operational and environmental conditions on board of the vessel were measured. Using these measurements, a statistical model has been created to calculate the power savings from the Flettner rotor.

The same vessel has been modelled in the Performance Prediction Program (PPP). Using the wind and ship speed as recorded by NAPA, the predicted power savings are calculated. In figure 3.21, the power savings are shown as reported by NAPA and as calculated by the PPP. The general distributions give a very good match: the average savings as reported by NAPA are 198 kW, the average as calculated by the PPP is 191 kW; a difference of only 4 %.

NAPA uses a statistical model in the analysis, based on the recorded on-board data. Taking in account possible measurement and modelling errors, the reported power savings by NAPA are an approximation of the actual savings. The fact that the PPP predicts very similar results, gives confidence in the accuracy of the PPP results.

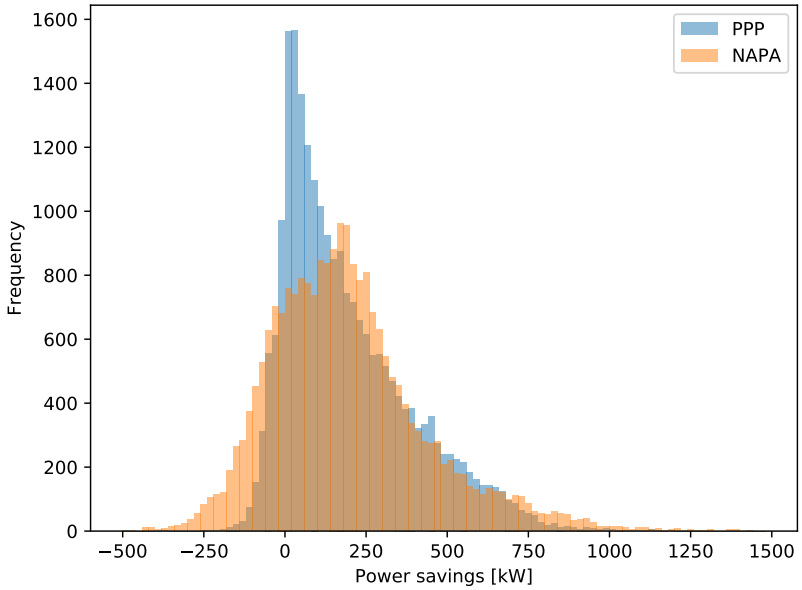

Figure 3.21: Power savings distribution as reported by NAPA and as calculated by the PPP. The frequency indicates the number of observations of power savings in any given range.

3.12. Conclusion and recommendations

This chapter describes the Performance Prediction Program (PPP), the model that is developed to determine the magnitude of all physical phenomena that are a result of Flettner rotors and to calculate the resulting fuel consumption.

The physical phenomena that are a result of Flettner rotors lead to a number of operational characteristics whose occurrence could affect the benefits of Flettner rotors. In section 3.2 an overview has been given of these operational characteristics, including measures that could be taken if they significantly affect the Flettner rotor fuel savings. The following operational characteristics have been identified. The next chapter discusses the method to determine their operational occurrence:

- To obtain heel and yaw balance, a ship with Flettner rotors is subjected to a heel angle and a rudder angle is applied. If those angles exceed operational limits, the Flettner rotors have to be throttled back, reducing their benefits.
- The side force production by the hull and rudder induces additional resistance, which has a negative contribution to the net Flettner rotor thrust.
- The thrust from Flettner rotors reduces the propeller and main engine load, changing their operating point and affecting their efficiency.

In sections 3.4 to 3.9, the methods for calculating all components included in the Performance Prediction Program (PPP) are described. It is shown that each individual component of the PPP gives accurate results; the same is true for the overall prediction of fuel savings.

It is shown that, in most practical cases, the PPP can accurately predict the fuel savings of a vessel equipped with Flettner rotors. Below, factors are listed that should be taken into account to ensure accurate results. To increase the applicability of the PPP, more research can be done in these areas.

- For several aspects of the PPP calculations, input from NAPA's reference vessel database is used. This database consists of vessel characteristics from a large range of cargo and passenger vessels. The aspects from NAPA's vessel database that are used in the PPP are the calm water resistance, added resistance in waves, specific fuel consumption and propulsion coefficients. If the user of the PPP wants to analyse vessels that are not in the range of NAPA's database, those aspects should be obtained in a different way.

- In section 3.4 it is assumed that rotors operate in uniform airflow. Rotors should be placed at a sufficient distance from cargo on deck, superstructures and other rotors to ensure undisturbed airflow to the rotors.
- In heel angle calculations small heel angles are assumed, which is generally valid (see section 3.5). In cases where larger heel angles occur, a heel angle limit can be specified to prevent inaccuracies in the results. This also prevents inaccurate hull side force predictions, as described in section 3.6.
- As described in section 3.7, some inaccuracies occur when calculating large rudder angles. In cases where larger rudder angles occur, a rudder angle limit can be specified to prevent inaccuracies in the results.

4

Weather Routing Program

In the previous chapter the Performance Prediction Program (PPP) is explained, which calculates the fuel consumption with and without Flettner rotors as function of vessel speed and wind conditions. In this chapter, this relationship is used to determine the annual fuel consumption of a vessel with Flettner rotors. For this, the Weather Routing Program (WRP) has been developed. This program uses results from the PPP, combined with historic weather data and vessel sailing schedules, to calculate the annual fuel consumption of a vessel. The WRP also provides the occurrence of the operational characteristics that were identified in chapter 3.

Section 4.1 provides the general structure and of the Weather Routing Program (WRP). In section 4.2 NAPA Voyage Optimization is described. Section 4.3 discusses how the WRP prepares voyage requests that will be analysed by NAPA Voyage Optimization. Section 4.4 discusses how the resulting output is processed to obtain the annual fuel savings and the influence of operational characteristics. In section 4.5, the influence of the implementation of the WRP on its results is discussed. Finally, in section 4.6 conclusions of this chapter are drawn.

4.1. Model description

In this research the Weather Routing Program (WRP) has been developed. Its basic structure and interaction with the Performance Prediction Program and NAPA Voyage Optimization is shown in figure 4.1. In the WRP voyage requests are created from the results from the Performance Prediction Program, a vessel's performance model and its sailing schedule. These voyage requests are then sent to NAPA Voyage Optimization, which returns the optimal voyages. The optimal voyages are processed in combination with the PPP results.

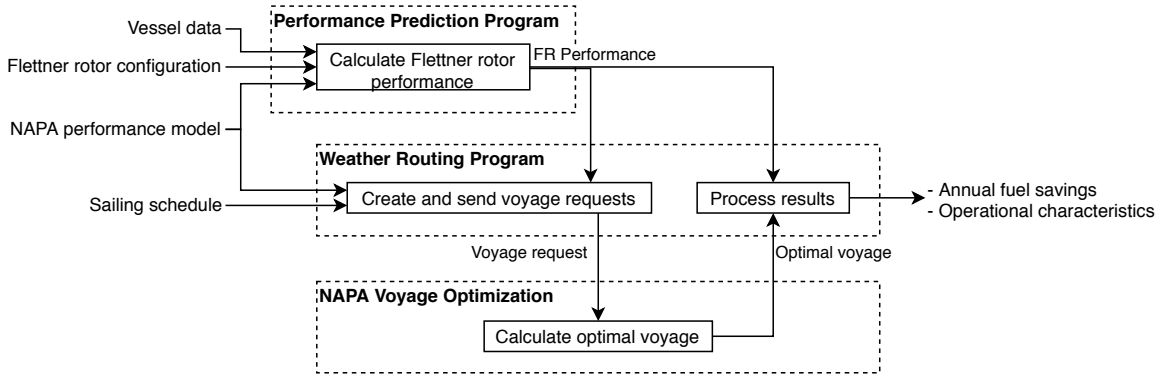

Figure 4.1: Basic structure of the Weather Routing Program

4.2. NAPA Voyage Optimization

For the operational analysis of vessels equipped with Flettner rotors, NAPA Voyage Optimization is used: weather routing software from NAPA, a Finnish maritime software, services and data analysis provider. For existing vessels, this software utilizes an accurate vessel simulation model in combination with up-to-date weather and sea current forecasts for efficient voyage planning. During this research, support for optimizing routes of vessels equipped with Flettner rotors was co-developed. This integration of Flettner rotors in NAPA Voyage Optimization will be explained in section 4.3.

4.2.1. NAPA performance model

NAPA Voyage Optimization uses historical wind, wave and current data to determine the expected fuel consumption during a voyage. To calculate the fuel consumption in these environmental conditions, a vessel's performance model is used. The performance model of a vessel consists of several tables, that correlate ship speed to calm water resistance, wind speed and direction to wind resistance and wave characteristics to added wave resistance. Also included are tables for propeller characteristics and for propulsion and engine efficiency. This allows for a straightforward calculation of the vessel's fuel consumption at any sailing speed in any wind, wave and current condition.

4.2.2. Optimisation algorithm

The optimisation algorithm in NAPA Voyage Optimization searches for the route for which vessel arrives at the desired arrival time, with the lowest possible fuel consumption. Two main assumptions are made to make the optimisation computations feasible. The first assumption is that the route of the vessel is split in separate legs. There is a grid of legs that limits number of possible routes that can be sailed. The second assumption is that the vessel sails with a fixed engine rotation speed along the whole route.

Route grid

NAPA Voyage Optimization uses a grid network of possible legs on a route, allowing for many different route variations. This grid discretization splits the voyage of a vessel in separate legs. On each leg, the ship speed and the environmental conditions are assumed to be constant for the duration that the vessel sails on that leg. With those constant speed and constant environmental conditions, the fuel consumption on each leg is calculated. In open seas, the grid network allows a vessel to sail in basically any direction. In areas where navigation is restricted, for example in shipping lanes or around offshore structures, the grid takes these restrictions into account. A typical transatlantic voyage consists of around 60 legs. In navigation restricted areas, the length of legs averages around 10 nm. In unrestricted areas, this average length is around 100 nm.

Constant engine speed

The second assumption that is made in NAPA Voyage Optimization, is that the vessel sails with a constant engine speed along the whole route. The optimisation algorithm searches for lowest possible constant engine speed, for which the vessel reaches its destination at the desired arrival time. Assuming a constant engine speed along the whole route reduces the amount of optimisation variables considerably, which makes the route optimisation computationally feasible.

When a high constant engine speed is required, on certain legs on the route with adverse weather conditions, the engine break power at this engine speed could exceed the maximum engine break power. In these situations, the engine speed is reduced until the the break power equals the maximum break power. This possibly results in later arrival times than desired.

4.2.3. Voyage data availability

Weather data is not available for all voyage simulations. As a result, in some cases no optimal route could be found by the algorithm. The availability of voyage data is on average higher in the summer period than in the winter period. *For this research, NAPA provided access to NAPA Voyage Optimization while the program was still under development. It is expected that this issue is resolved at the time this research is published.*

4.2.4. Optimal voyage
NAPA Voyage Optimization outputs many details of the calculated optimal voyage. For each leg on the voyage the output consists of the start and end locations of the leg, the times at which the vessel passed these locations, the ship speed, propeller rotation speed and fuel consumption during the leg and the encountered environmental conditions: wind, waves and current.

4.3. Voyage requests
The input for NAPA Voyage Optimization is a so-called voyage request. This request contains all information that is required to determine the optimal route for a vessel with Flettner rotors. It consists of two parts: a vessel's performance model and details of one voyage in a vessel's sailing schedule.

4.3.1. Flettner rotor effects in performance model
For the evaluation of the effects of Flettner rotors in NAPA Voyage Optimization, NAPA has implemented the functionality to add an additional input table to a vessel's performance model. In this table the forces in surge direction have to be provided as a function of vessel speed, true wind speed and true wind direction. The force that is included in the performance model table is the rotor net thrust force $X_{FR,net}$; the sum of all components from equation (3.1) that are a direct consequence of the Flettner rotors.

$$X_{FR,net} = X_{FR} + R_{i,H} + R_{i,R} \tag{4.1}$$

where X_{FR} is the rotor thrust, $R_{i,H}$ is the induced hull resistance and $R_{i,R}$ is the induced rudder resistance as defined in equations (3.12), (3.16) and (3.27), respectively. By using the net thrust force, the rotor thrust that is used in the voyage simulations is corrected for the negative effects of Flettner rotors on the x-force balance.

In NAPA Voyage optimization, this rotor net thrust force is treated as an additional resistance component when determining the fuel consumption in any weather condition along the route.

4.3.2. Sailing schedule
A vessel's sailing schedule is a list of voyages, where for each voyage the times and locations of departure and arrival are specified. For voyage in this list, a voyage request will be sent to NAPA Voyage Optimization. Two different methods can be used to generate a vessel's sailing schedule: an actual sailing schedule can be used, or a schedule is generated based on typical voyages.

Historic sailing schedules
When the actual historic sailing schedule of a vessel is known, each voyage from this schedule is simulated in NAPA Voyage Optimization. When the historic sailing schedule consists of several years of voyages, this will result in a very accurate representation of the operational profile of a vessel. This operational profile will show the actual sailing speed distribution and vessel occupation, resulting in a representative prediction for the fuel savings, which is used to determine the payback period of the Flettner rotor investment.

Typical voyages
When the actual sailing schedule of a vessel is not known, one or more typical voyages can be used to create a schedule. The schedule will consists of the many repetitions of same voyage or set of voyages, each repetition with a different departure time. The different departure times cover a large time period to get a good representation of the different environmental conditions that are encountered.

Voyage Requests without Flettner Rotors
Besides the voyage requests as described above, the same requests are sent a second time. This second time, the effects of Flettner rotors are removed from the performance model. This results in the optimal voyages for when no Flettner rotors would have been installed on the vessel. This allows for properly comparing the fuel consumption of a vessel with and without Flettner rotors.

4.4. Post-processing results

When all voyage requests from a sailing schedule are processed by NAPA Voyage Optimization, the results are post-processed by the Weather Routing Program. First, the fuel consumption from the Flettner Rotors is added to each voyage, followed by calculating the fuel savings from the Flettner rotors. The last post-processing step is to calculate and show the distribution of operational characteristics.

4.4.1. Flettner rotor fuel consumption

In NAPA Voyage Optimization it is currently not possible to add the Flettner rotor fuel consumption (equation (3.64)) as an input to the performance model. The results of the NAPA Voyage Optimization contain the main engine fuel consumption on each leg of the optimal route, as well as the weather conditions. During post-processing of the NAPA Voyage Optimization results, the Flettner rotor fuel consumption is calculated. For each leg on the route, the weather conditions are used to determine the rotor fuel consumption. To obtain the total fuel consumption on a leg, the rotor fuel consumption is added to the main engine fuel consumption as determined in the Voyage Optimization. Summing the total fuel consumption of each leg gives the total fuel consumption on a voyage.

4.4.2. Annual fuel savings

Each voyage in the sailing schedule is simulated twice; once with and once without Flettner rotors (see section 4.3.2). The total fuel consumption for both simulations is compared, which results in the fuel savings from the Flettner rotors on that voyage. When actual sailing schedules are simulated, the expected annual fuel savings are sum of the savings on each voyage in a simulated year. When one or more typical voyages are simulated repeatedly, the average savings on this (set of) voyage(s) is used to estimate the total annual fuel savings.

4.4.3. Operational characteristics

Similar to the rotor fuel consumption, also other operational characteristics are determined for each leg on each voyage. Depending on the specific application, the operational characteristics of interest could include the thrust delivered by the Flettner rotors, heel angles, rudder angles required to keep course and the main engine load.

An example of the thrust contribution from Flettner rotors on a transatlantic voyage is shown in figure 4.2. This example clearly shows the different optimal routes for the same ship with and without Flettner rotors.

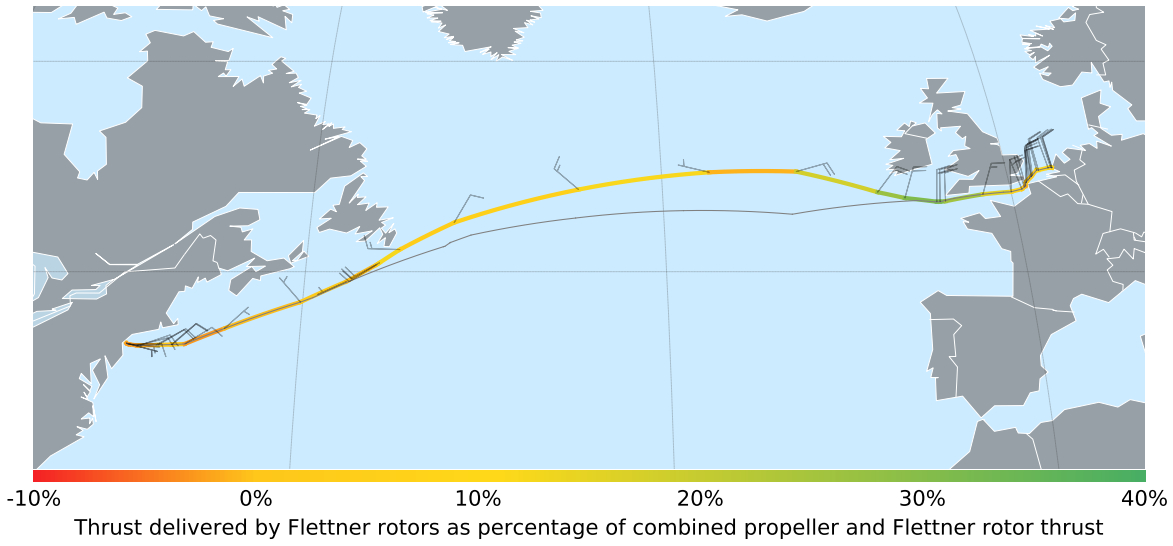

Figure 4.2: Weather routing output. Optimal route example between Rotterdam and New York for the M/V Estraden with two 30 m by 5 m Flettner rotors (coloured) and without Flettner rotors (grey). Particulars of the M/V Estraden are shown in table 3.1

The Weather Routing Program provides the distribution of the operational characteristics over all simu-

lated voyages. This can provide useful information during a vessel's concept design stage. For example, the occurrence of undesirably large rudder angles or heel angles could be compared for vessels with different Flettner configurations.

Another example of useful information in a concept concept design stage follows from the engine load distribution. When the occurrence of high engine loads is significantly higher on the vessel with Flettner rotors compared to the vessel without Flettner rotors, the vessel's designer could consider installing a smaller main engine, reducing the building costs of the vessel. The new vessel design, with smaller engine, can also be analysed by the and WRP to see if this adjusted design still is able to arrive at the desired arrival time on all voyages.

4.5. WRP discussion

In the previous sections, several aspects of the Weather Routing Program have been mentioned that could be improved. The effects of the current WRP implementation are discussed below.

4.5.1. Historical data

NAPA Voyage Optimization is based on historical weather data: the calculated optimal voyage is the optimal voyage that could have been sailed. In practice, the voyage optimisation uses predicted weather conditions and determines the expected optimal route. The actual savings could therefore be lower than predicted, especially on longer routes where weather predictions have a higher degree of uncertainty.

4.5.2. Flettner rotor fuel consumption

As explained in section 4.4, the rotor fuel consumption is currently not taken into account in finding the optimal route with the lowest fuel consumption. This means that the optimal route is optimised for the lowest main engine fuel consumption, not for the total fuel consumption. The effect of this is that there can exist even more optimal routes than predicted by NAPA Voyage Optimization. This effect is expected to be limited, since the rotor fuel consumption generally does not exceed 5% of the total fuel consumption.

4.5.3. Voyage data availability

As explained in section 4.2.3, not all voyage simulation results are available. The effects of the lower voyage data availability is discussed below.

Effects on fuel savings and operational characteristics

As explained in section 4.2.3, on average more voyage data is available in the spring and summer period than in the fall and winter period. On average higher wind speeds occur in the fall and winter period. In general, higher wind speeds lead to larger fuel consumption savings from Flettner rotors. As a consequence, it is expected that, on voyages for which the results are unavailable, the fuel savings from Flettner rotors are higher than average. Therefore, a lower availability of voyage data leads to a higher degree of underestimation of the expected fuel consumption savings.

Similarly at higher wind speeds, also higher rudder angles and higher heel angles occur. The occurrence of high rudder and heel angles is therefore also underestimated with lower availability of voyage data.

Effects of reduced main engine size

A possible benefit of installing Flettner rotors is that the main engine size can be reduced without reducing the average sailing speed. The results of the WRP show if the ship is able to arrive at the destination without delays. This can be used in assessing the trade-off between the investment in engine size (and all related systems) and the earning capacity of a vessel. For example, the WRP can be used to analyse how much the installed engine power can be reduced while still being able to maintain a predefined sailing schedule.

On average, such delays in arrival time will occur more on voyages in the winter seasons. These are the same voyages for which the voyage data availability is lower, as explained in section 4.2.3. This means that a part of the arrival time delays will not be shown in the analysis results.

For a large number of the voyages, the voyage data will be available, both with and without Flettner rotors, both with and without engine size reduction. On these voyages the effect of an engine size reduction on the arrival time delays can be determined. On the voyages however for which the simulation data is unavailable, this effect on the arrival times is expected to be the most significant. This means that no data about arrival time delays is available for those voyages for which the likelihood of arrival time delays is the largest. Consequently, no conclusions can be drawn from these voyages.

4.6. Conclusion

The Weather Routing Program (WRP) is shown to provide good method to predict the annual fuel consumption savings of a vessel. The WRP combines the Flettner rotor performance from the Performance Prediction Program, a Performance model from NAPA and a sailing schedule to create voyage requests. The WRP sends those voyage requests to NAPA Voyage Optimization, which calculates the optimal route with the lowest fuel consumption. The WRP then processes these optimal voyages to provide annual fuel savings and the distribution of operational characteristics.

Combined with the other cost categories that are mentioned in chapter 2, the annual fuel savings can be used to calculate the payback period of a Flettner rotor investment.

The Weather Routing Program provides information about the distribution of operational characteristics, which can be used to identify aspects of a ship design that can be optimised to increase the benefits of Flettner rotors. A case study will illustrate this in chapter 5.

Three aspects of the WRP have been identified that affect the WRP results. The first effect rises from the fact that historical weather data is used in the optimisations, the second effect from the fact that Flettner rotor fuel consumption is not taken into account in the optimisation algorithm. The first effect leads to a small overestimation of the annual fuel consumptions savings from Flettner rotors, while the second effect leads to a small underestimation of those savings. Together, those effects are expected to not have a significant impact on the payback period of Flettner rotors.

The third aspect of the current WRP implementation that affects its results, is that a part of the voyage results data is unavailable. The voyage data availability is lower on voyages where the fuel consumption savings from Flettner rotors are likely to be higher. This leads to a underestimation of the expected fuel savings and occurrence of high values in heel and rudder angles.

Another effect of voyage data unavailability is that the influence of engine size reductions is hard to asses. The same voyages that are likely to be affected by a decrease in engine size, are also the voyages for which the voyage data is less likely to be available. This inhibits the analysis of effects of an engine size reduction on those voyage.

5

Case study

This chapter describes a case study that is performed to demonstrate how this research is applied. A potential client of C-Job Naval Architects showed interest in installing a Flettner rotor on a new ship. Section 5.1 describes the ship design and two potential Flettner rotor configurations. Section 5.2 discusses the fuel savings obtained by Flettner rotors in this case study and section 5.3 discusses the effects on the operational characteristics.

5.1. Case ship

A potential client of C-Job Naval Arcitects has interest in adding a $4\,000$ DWT general dry cargo ship to its fleet and wants to explore the effects of installing a Flettner rotor. The initial concept design of this ship is used to perform performance calculations with the methods developed in this research. The main particulars of this design are shown in table 5.1

Table 5.1: Case ship particulars and rotor configurations

Case ship particulars		
Length over all	96.0	m
Breadth	13.0	m
Draught	5.5	m
DWT	4 000	ton
Propulsion power	1 200	kW
Design service speed	10	kt

Rotor configurations	Rotor front	Rotor Aft	
(x, y, z) from (APP, CL, BL)	(80, 0, 16)	(0, 0, 10)	m
Rotor height	24	24	m
Rotor diameter	4	4	m

The vessel owner has interest in one 24 m by 4 m Flettner rotor, that can either be installed on the aft deck of the ship or on the front of the ship on top of the bridge. Both Flettner rotor configurations are analysed with the Performance Prediction Program that is described in chapter 3. The resulting Flettner rotor performance is used as input for the Weather Routing Program that is described in chapter 4. No sailing schedule is known yet for the concept ship, so the operational simulations will be based on the expected most frequently sailed route: from Rotterdam to Casablanca and back. Using historic weather data, with each Flettner rotor configuration 48 round trips have been simulated over the course of 2018. Also reference simulations have been performed for the same ship without Flettenr rotors. In each single voyage simulation the NAPA Voyage Optimization algorithm is used to minimise the fuel consumption, while still arriving within 180 hours (7.5 days) after departure.

5.2. Fuel savings

Table 5.2 shows the fuel savings per voyage, averaged over all simulated voyages. Higher fuel savings are obtained with the Flettner rotor installed on the front of the vessel than with the Flettner rotor on the aft. On average 3.6 t on fuel is saved on a round trip with the Flettner rotor on the front, a reduction of 12.9 %. With the rotor on the aft, 11.6 % fuel is saved.

With twenty round trips annually and a fuel price of $ 600 per ton, the annual fuel cost savings are $ 43 000 per year for the configuration with the Flettner rotor at the front. With initial investment costs of $ 650 000 [9] the payback period of this investment is 15 years. Flettner rotor maintenance costs and other additional costs mentioned in chapter 2 are not yet taken into account in this calculation.

Table 5.2: Average Flettner rotor (FR) fuel oil consumption (FOC) per voyage between Rotterdam and Casablanca

Route	Rotor location	FOC with FR [t]	FOC without FR [t]	Savings [%]	Savings [t]
RDM-CAS	Front	10.0	12.2	17.0	2.1
RDM-CAS	Aft	10.1	12.2	16.3	2.0
CAS-RDM	Front	14.3	15.8	9.8	1.5
CAS-RDM	Aft	14.6	15.8	8.2	1.2

As explained in section 4.5, a part voyage simulation data is unavailable. This can clearly be seen in figure 5.1. In each month four voyages were simulated, but only the available simulation data are shown in the figure. The availability of voyage data is higher in the spring and summer period than in the fall and winter. In this same period fuel savings are lower on average. This suggests that the fuel savings that are presented in table 5.2 are lower than the actual savings that could be obtained when all voyage data would be available.

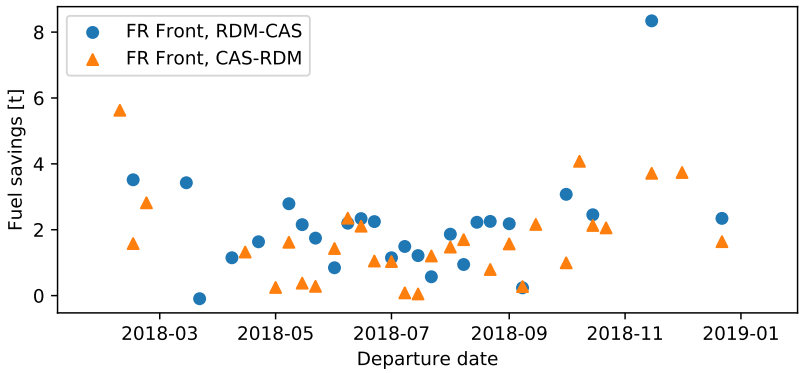

Figure 5.1: Fuel savings per successfully simulated voyage with the Flettner rotor on the front of the case ship

5.3. Operational characteristics

In section 3.2 the operational characteristics are introduced that are affected by Flettner rotors or have an effect on the benefits of Flettner rotors. For both rotor configurations, the distribution of the operational characteristics along all simulated voyages is determined using the method that is explained in section 4.4. The distribution plots of all operational characteristics are shown in appendix A.

5.3.1. Rudder angles

The most notable difference in operational characteristics between both Flettner rotor configurations is the difference in rudder angle occurrence, see figure 5.2. The required rudder angles to keep a straight course are significantly larger in the configuration with the Flettner rotor on the aft of the ship. This leads to a larger rudder resistance, as can be seen in figures 5.3 and 5.4. This is the main cause of the lower fuel savings of this Flettner rotor configuration.

When the large rudder angles in the configuration with the Flettner rotor on the aft of the vessel are

considered to be too large, the Flettner rotor could be throttled back. This reduces the rotor side force and reduces the required rudder angle. However this also reduces the rotor thrust, and therefore the fuel savings will be lower in this rotor configuration. To quantify this reduction in fuel savings, a second iteration could be done with the Performance Prediction Program and the Weather Routing Program, in which a rudder angle limit is applied.

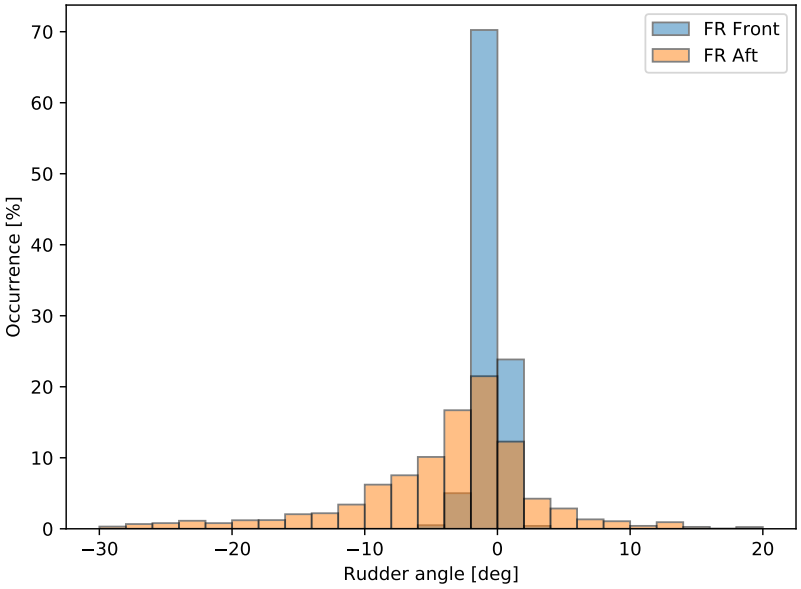

Figure 5.2: Rudder angle, occurrence over all simulated voyages for both Flettner rotor (FR) configurations

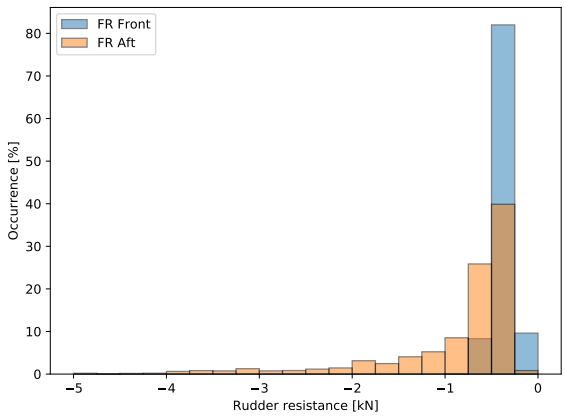

Figure 5.3: Rudder resistance, occurrence over all simulated voyages for both Flettner rotor (FR) configurations

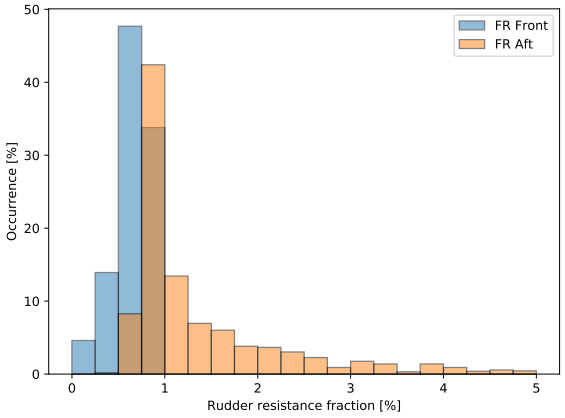

Figure 5.4: Rudder resistance relative to the total resistance, occurrence over all simulated voyages for both Flettner rotor (FR) configurations

5.3.2. Heel angles

The potential client for this case study expressed concern for the occurrence of high heel angles in the configuration where Flettner rotor is placed in the front of the ship, on top of the bridge. Figure 5.5 shows the heel angles for both rotor configurations. As expected, the heel angles are larger in the configuration with the Flettner rotor on top of the bridge. However, the heel angles do rarely exceed 2°, so they are no reason for concern.

The configuration with the Flettner rotor at the front of the ship leads to higher fuel savings and lower required rudder angles compared to the configuration with the Flettner rotor at the aft, while not resulting in any considerable negative effects. Therefore this configuration is considered to be the best option

for this case study.

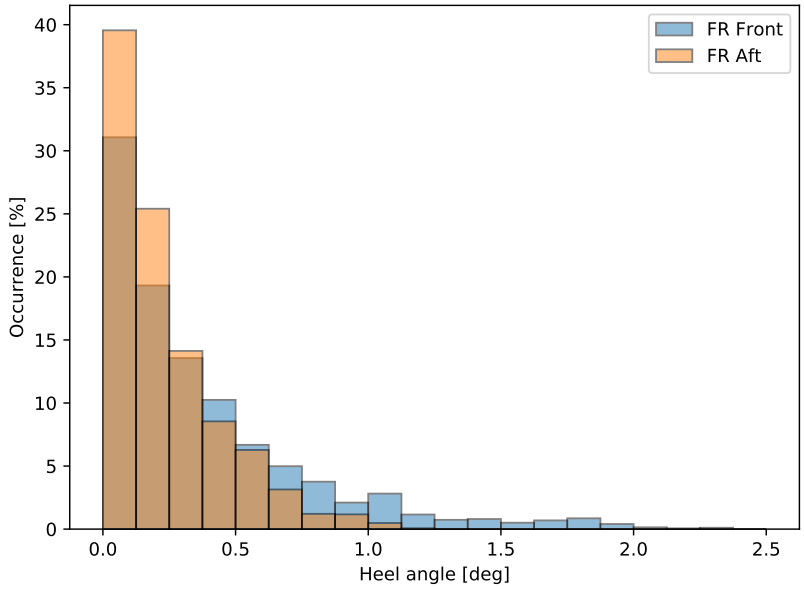

Figure 5.5: Heel angle, occurrence over all simulated voyages for both Flettner rotor (FR) configurations

5.3.3. Additional resistance

In the configuration with the Flettner rotor on the front of the ship, the induced rudder and hull resistances both never exceed 2 % of the ship's total resistance during all simulated voyages. Improvements in the efficiency of side force production by the rudder and the hull would have limited effect on the fuel savings from the Flettner rotor. Therefore it is considered that it is not necessary to optimise the ship design for reducing the rudder and hull induced resistance.

5.3.4. Propulsion efficiency

This subsection discusses the operational characteristics regarding the propulsion efficiency: propeller open water efficiency, main engine load and specific fuel consumption. These characteristics show no significant differences between both Flettner rotor configurations (figures A.18, A.19 and A.20). The effect of Flettner rotors on these operational characteristics is best illustrated by comparing them with the operational characteristics of the case ship without Flettner rotors.

Open water efficiency

Figure 5.6 shows the distribution propeller open water efficiency for both the ship without Flettner rotors and with the Flettner rotor installed on the front of the vessel. In both cases, the propeller generally operates below its optimal operating point. Whether or not the client chooses to install a Flettner rotor on the ship, the propeller should be better matched to the operational conditions. One explanation of the low average open water efficiency is that the propeller operates at a relatively low advance ratio, since the average sailing speed in the simulations is 8 kt, while the ship's design speed is 10 kt.

The ship with Flettner rotor generally operates with a higher open water efficiency than the ship without Flettner rotor. This is is caused by a higher propeller advance ratio due to the lower thrust requirement.

Engine efficiency

Figure 5.7 shows that generally the ship sails with a low main engine load, both with and without Flettner rotor. This leads to a relatively high specific fuel consumption, as can be seen in figure 5.8. This suggests that the main engine design could be better matched to the operating conditions in a later design stage. One explanation of the low average engine load is that the average sailing speed in the simulations is 8 kt, while the ship's design speed is 10 kt.

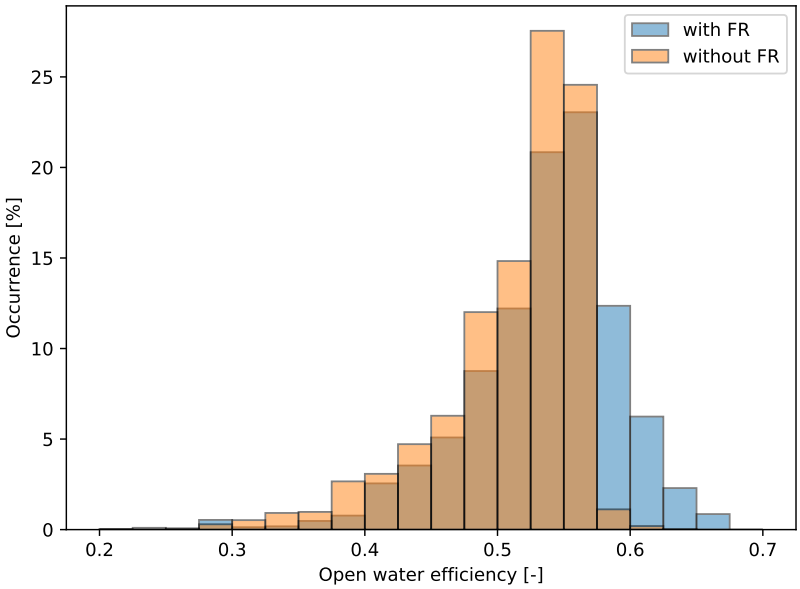

Figure 5.6: Propeller open water efficiency, occurrence over all simulated voyages with a Flettner rotor (FR) on the front and without Flettner rotor

On average, the main engine load with a Flettner rotor on the front of the ship is $18\,\%$ lower than without Flettner rotor. This indicates that installing a Flettner rotor could allow for reducing the installed main engine power. This leads to building cost reductions that increase the payback period of the Flettner rotor.

The availability of the voyage simulation data is lower in the fall and winter months. Therefore the actual average engine loads are expected to be higher. This is expected for the configurations both with and without Flettner rotors, since more wave added resistance is expected in these periods. However, the engine load increase is expected to be less significant for the ship with Flettner rotor, since also the Flettner rotor thrust is expected to increase in the fall and winter period with higher average wind speeds. Therefore, with the current voyage simulation availability, no quantitative conclusions can be drawn from the simulation results.

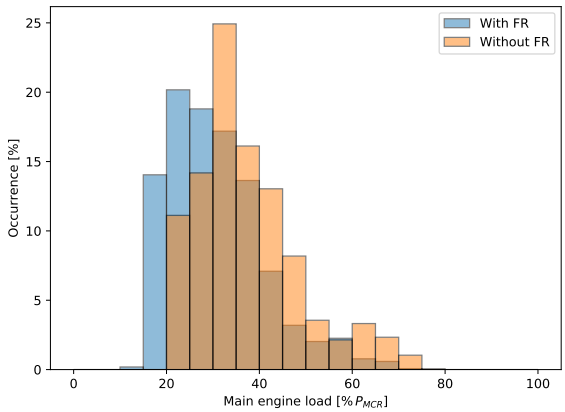

Figure 5.7: Main engine load, occurrence over all simulated voyages with a Flettner rotor (FR) on the front and without Flettner rotor

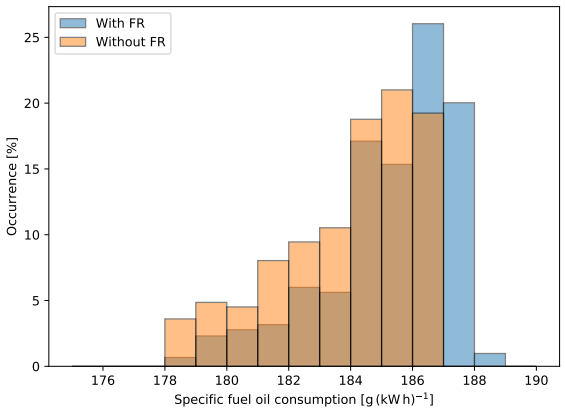

Figure 5.8: Main engine specific fuel consumption, occurrence over all simulated voyages with a Flettner rotor (FR) on the front and without Flettner rotor

5.4. Conclusion

This chapter illustrated the use of the Performance Prediction Program and the Weather Routing Program by performing a case study of installing a Flettner rotor on a $4\,000$ DWT general dry cargo ship. Two locations for the Flettner rotor were considered: on the front or on the aft of the ship. The configuration with the Flettner rotor on the front showed to provide the highest fuel savings of $12.9\,\%$. The resulting investment payback period is 15 years. This is expected to be a conservative estimate due to the unavailability of some voyage data.

Analysis of the operational characteristics showed that the position of the Flettner rotor has a significant impact on the rudder angles that are required to keep a straight course. Significantly lower rudder angles are required for the configuration with the rotor on the front, compared to the configuration with the rotor on the aft of the ship. The rudder angles could be reduced by throttling back the Flettner rotor, but this also reduces the rotor's benefits. The operational characteristics for heel and additional resistance due to the Flettner rotor showed no significant effects.

The operational analysis of the propulsion efficiency showed that both the propeller and the main engine generally operate below their most efficient point. One of the reasons for this is that average sailing speed at the simulated voyage lays below the ship's design speed.

The average main engine load is reduced by $18\,\%$ as a result of the Flettner rotor. This potentially allows for installing a smaller main engine. However, a part of the voyage data was unavailable, leading to biased engine load results. Therefore, the presented results do not provide sufficient information for optimally matching the propeller and engine design to the operational conditions.

6

Conclusions and recommendations

To stimulate the uptake of the application of Flettner rotors, the uncertainty of their economic benefits needs to be reduced. Therefore, in this report the following research question has been answered:

> How can the aspects of a vessel design be identified, that can be optimised to minimise the payback period of Flettner rotors?

The following section consists of the research's sub-questions and their answers, that together answer the main research question. This chapter's last section discusses the most important recommendations for further research.

6.1. Conclusions

In chapter 2, the influence of Flettner rotors on the different aspects of a vessel's total cost of ownership have been discussed, answering the first sub-question:

1. What aspects of the total cost of ownership of a vessel are affected by the application of Flettner Rotors?

The main cost categories that are affected are the building costs and the fuel consumption. The building costs are increased by the purchase and installation of the rotors themselves, and by potential design optimisations to increase the rotor benefits. In an early design stage, estimation methods are available for those costs. Estimating the fuel consumption savings however, is significantly harder.

The first step of determining the fuel consumption savings is described in chapter 3, where the second sub-question is answered:

2. How can the effect of Flettner rotors on the fuel consumption be quantified?

The Performance Prediction Program (PPP) has been developed during this research. The PPP determines the fuel savings of a vessel equipped with Flettner rotors in any wind condition. This is done by solving the force and moment balance equations in surge, sway, roll and yaw directions, including the physical effects from Flettner rotors. It is shown that the PPP provides accurate results, in close comparison to on-board measurements.

The second step of determining the fuel consumption savings from Flettner rotor to determine their payback period, is described in chapter 4, answering the third sub-question:

3. How can voyage optimisation be applied to calculate the annual fuel savings from Flettner rotors?

For answering this question, the Weather Routing Program (WRP) has been developed. The WRP uses results from the PPP, combined with historic weather data and vessel sailing schedules, to calculate the annual fuel consumption of a vessel. The WRP sends voyage requests to NAPA Voyage Optimization, which calculates the optimal route with the lowest fuel consumption for each voyage.

Due to the current implementation of the WRP, a part of the voyage data is unavailable. This leads to an underestimation of the expected annual fuel savings from Flettner rotors.

In chapter 4 also the answers the fourth and last sub-question:

4. How can the influence of operational characteristics on the benefits from Flettner rotors be determined?

Besides the fuel consumption savings, the Weather Routing Program also calculates the distribution of operational characteristics like heel angles, rudder angles and engine load. These characteristics can be used to identify aspects of a vessel that could be optimised to increase the benefits form Flettner rotors. Due to the current implementation of the WRP, the occurrence of operational characteristics like high heel and rudder angles is underestimated. The results of the WRP still allow for a qualitative comparison of these characteristics between different vessel design variations.

Chapter 5 shows how this research can be used to answer the main research question. A case study is performed in which three aspects of a the ship design were identified that can be optimised to minimise the payback period of Flettner rotors:

- It was shown that the position of the Flettner rotor on the ship has significant influence on the operational occurrence of large rudder angles. Choosing the optimal Flettner rotor location ensures adequate manoeuvring capabilities for the ship.
- The operational analysis of propeller efficiency showed that the propeller often not operates near its optimal operating point. Much can be gained from properly matching the propeller to the operational conditions.
- Similar to the propeller, the main engine should be better matched to the operational conditions to improve its average efficiency. Even more, the operational analysis showed that the average main engine load is significantly reduced as a result of Flettner rotors. This possibly allows to install a smaller main engine. This could reduce the Flettner rotor investment cost and decrease the investment payback time.

Just as important is the fact that a number of design aspects were identified for which optimisation has *no* significant effect on the payback period of Flettner rotors:

- Heel angles do not reach any comfort or safety limits, so no measures have to be considered to increase the ship's stability.
- Rudder angles are reduced to acceptable levels with the Flettner rotor on its optimal position. Therefore no other measures are required to increase manoeuvring capabilities; no larger or more effective rudders are required, additional appendages do not have to be considered.
- The rudder and hull side force induced resistance are small compared to the Flettner rotor thrust, so the hull and rudder do not need to be optimised to increase the efficiency of side force production.

6.2. Recommendations

The Performance Prediction Program (PPP, see chapter 3) can generally be used to predict the performance of Flettner rotors on a large range of vessels. Currently the several factors need to be taken into account to ensure accurate results from the PPP:

- Flettner rotors should be placed at sufficient distance from cargo, superstructures and other rotors to prevent interaction effects that are not taken into account in the PPP.
- The PPP provides accurate results for small heel angles and small rudder angles. This valid range of heel and rudder angles corresponds to angles that are generally acceptable on board of vessels. If the PPP is to be used for vessels that allow for larger heel and/or rudder angles, more research is required.

As discussed in chapter 4, in the current implementation of the Weather Routing Program (WRP) a part of the voyage simulation data is unavailable. This leads to several inaccuracies in the fuel savings prediction and in the distribution of operational characteristics like rudder angles and engine load. The WRP is currently not able to provide accurate information for assessing the advantages and disadvantages of potential main engine size reductions. Further research is required to improve the availability of voyage simulation data.

Bibliography

[1] C. Badalamenti and S. Prince. Effects of Endplates on a Rotating Cylinder in Crossflow. In *26th AIAA Applied Aerodynamics Conference*, Honolulu, Hawaii, 2008. American Institute of Aeronautics and Astronautics. doi: doi:10.2514/6.2008-706310.2514/6.2008-7063. URL https://doi.org/10.2514/6.2008-7063.

[2] M.M. Barnitsas, D. Ray, and P. Kinley. Kt, Kq and Efficiency Curves for the Wageningen B-Series Propellers. Report 237, University of Michigan, 1981-05-01 1981.

[3] K.C.-v.d. Boom. Dnv Gl Issues Norsepower First-Ever Design Type Approval for Onboard Wind Propulsion System, 03-05-2019 2019. BLUE Communications. URL https://www.norsepower.com/news/dnv-gl-issues-norsepower-first-ever-design-type-approval-for-onboard-wind-propulsion-system.

[4] G. Bordogna, S. Muggiasca, S. Giappino, M. Belloli, J.A. Keuning, R.H.M. Huijsmans, and A.P. van 't Veer. Experiments on a Flettner Rotor at Critical and Supercritical Reynolds Numbers. *Journal of Wind Engineering and Industrial Aerodynamics*, 188:19–29, 2019. ISSN 01676105. doi: 10.1016/j.jweia.2019.02.006.

[5] A. Burden, T. Lloyd, S. Mockler, L. Mortola, I.B. Shin, and B. Smith. Concept Design of a Fast Sail Assisted Feeder Container Ship. Report, University of Southampton, 2010. URL https://eprints.soton.ac.uk/173137/.

[6] A. De Marco, S. Mancini, C. Pensa, G. Calise, and F. De Luca. Flettner Rotor Concept for Marine Applications: A Systematic Study. *International Journal of Rotating Machinery*, 2016:12, 2016. ISSN 1023-621X 1542-3034. doi: 10.1155/2016/3458750. URL http://dx.doi.org/10.1155/2016/3458750.

[7] R. Eggers. Operational Performance of Wind Assisted Ships. In *10th Symposium on High-Performance Marine Vehicles (HIPER)*, pages 366–379, 2016. URL http://www.marin.nl/web/Publications/Publication-items/Operational-Performance-of-Wind-Assisted-Ships.htm.

[8] L. George. Shipping Fuel Costs to Spike 25 Percent in 2020 on Sulfuric Cap: Woodmac. *Reuters*, 2018. URL https://www.reuters.com/article/us-shipping-fuel-costs/shipping-fuel-costs-to-spike-25-percent-in-2020-on-sulfuric-cap-woodmac-idUSKBN1HI1AT.

[9] GloMEEP. Flettner Rotors, 2019. Global Maritime Energy Efficiency Partnerships. URL https://glomeep.imo.org/technology/flettner-rotors/.

[10] J. Holtrop. A Statistical Re-Analysis of Resistance and Propulsion Data. *International Shipbuilding Progress*, 31:272–276, 1984.

[11] M. Insel and A. Olcer. Speed-Resistance-Power Prediction for 3000 Dwt Coaster in Sailing Conditions. Report, World Maritime University, 2015.

[12] D. Kang and K. Hasegawa. Prediction Method of Hydrodynamic Forces Acting on the Hull of a Blunt-Body Ship in the Even Keel Condition. *Journal of Marine Science and Technology*, 12(1): 1–14, 2007. ISSN 1437-8213. doi: 10.1007/s00773-006-0232-7. URL https://doi.org/10.1007/s00773-006-0232-7.

[13] K. Kijima, T. Katsuno, Y. Nakiri, and Y. Furukawa. On the Manoeuvring Performance of a Ship with the Parameter of Loading Condition. *Journal of the Society of Naval Architects of Japan*, 1990 (168):141–148, 1990. doi: 10.2534/jjasnaoe1968.1990.168_141.

[14] K. Kijima, Y. Nakiri, and Y. Furukawa. On a Prediction Method for Ship Manoeuvrability. In *International workshop on ship manoeuvrability - 25 years CPMC at HSVA*, 2000. URL http://mararchief.tudelft.nl/file/5941/.

[15] J. Liu and R. Hekkenberg. Sixty Years of Research on Ship Rudders: Effects of Design Choices on Rudder Performance. *Ships and Offshore Structures*, 12(4):495–512, 2017. ISSN 1744-5302. doi: 10.1080/17445302.2016.1178205. URL https://doi.org/10.1080/17445302.2016.1178205.

[16] J.-F. Masset. Power Required to Rotate a Cylinder with End Plates in a Moving Air, 26-10-2018 2018. URL https://www.boatdesign.net/threads/flettner-rotors-calculating-rotating-skin-friction.60516/.

[17] E. Mobron. Improving a Sail-Assisted Cargo Vessel's Hull. *SWZ Maritime*, February 2015.

[18] A.F. Molland and S.R. Turnock. Wind Tunnel Tests on the Effect of a Ship Hull on Rudder-Propeller Performance at Different Angles of Drift. Report, University of Southampton, 1995. URL https://eprints.soton.ac.uk/46045/.

[19] A.F. Molland and S.R. Turnock. 5 - Experimental Data, pages 71–232. Butterworth-Heinemann, Oxford, 2007. ISBN 978-0-7506-6944-3. doi: https://doi.org/10.1016/B978-075066944-3/50008-1. URL http://www.sciencedirect.com/science/article/pii/B9780750669443500081.

[20] L. Moskowitz. Estimates of the Power Spectrums for Fully Developed Seas for Wind Speeds of 20 to 40 Knots. *Journal of Geophysical Research (1896-1977)*, 69(24):5161–5179, 1964. doi: doi:10.1029/JZ069i024p05161. URL https://agupubs.onlinelibrary.wiley.com/doi/abs/10.1029/JZ069i024p05161.

[21] T. Nikkels. Ecoliner - Future Design in Progress. Report, Dykstra Naval Architects, 2013. URL http://www.marin.nl/web/file?uuid=000bd829-eeea-4479-bc80-a1ba27fc8cb4&owner=bbe0c94c-375d-4ae8-b452-251a414c25d7.

[22] Norsepower. M/V Estraden, 2019. URL https://www.norsepower.com/ro-ro.

[23] Norsepower. Technical Specifications, 2019. Norsepower Oy Ltd. URL https://www.norsepower.com/for-designers.

[24] J. Norwood. Rotors Revisited. *Catalyst, Journal of the Amateur Yacht Research Society*, 5, 2001.

[25] H.J. Pijl. Application of Flettner Rotors on Modern Freighters. Report, C-Job Naval Architechts, 2015.

[26] N. Rehmatulla, S. Parker, T. Smith, and V. Stulgis. Wind Technologies: Opportunities and Barriers to a Low Carbon Shipping Industry. *Marine Policy*, 75:217–226, 2017. ISSN 0308-597X. doi: https://doi.org/10.1016/j.marpol.2015.12.021. URL http://www.sciencedirect.com/science/article/pii/S0308597X15003917.

[27] E.G. Reid. Tests of Rotating Cylinders. Report NACA-TN-209, National Advisory Committee for Aeronautics, 1924.

[28] V.L. Russo and K. Sullivan. Design of the Mariner-Type Ship. *Transactions of The Society of Naval Architects and Marine Engineers*, 61:98–151, 1953.

[29] H. Schneekluth and V. Bertram. Main Dimensions and Main Ratios, book section 1, pages 1–33. Butterworth-Heinemann, Oxford, 1998. ISBN 978-0-7506-4133-3. doi: https://doi.org/10.1016/B978-075064133-3/50001-3. URL http://www.sciencedirect.com/science/article/pii/B9780750641333500013.

[30] J. Seifert. A Review of the Magnus Effect in Aeronautics. *Progress in Aerospace Sciences*, 55:17–45, 2012. ISSN 0376-0421. doi: https://doi.org/10.1016/j.paerosci.2012.07.001. URL http://www.sciencedirect.com/science/article/pii/S0376042112000656.

[31] C.D. Simonsen. Rudder, Propeller and Hull Interaction by Rans. Technical University of Denmark (DTU), Kgs. Lyngby, Denmark, 2000.

[32] T. Smith, J. P. Jalkanen, B. A. Anderson, J. Corbett, J. Faber, S. Hanayama, E. O'Keeffe, S. Parker, L. Johansson, L. Aldous, C. Raucci, M. Traut, S. Ettinger, D. Nelissen, D. Lee, S. Ng, A. Agrawal, J. Winebrake, M. Hoen, and A. Pandey. Third Imo Ghg Study 2014. Report, International Maritime Organization (IMO), 2015. URL http://www.imo.org/en/OurWork/Environment/PollutionPrevention/AirPollution/Documents/Third%20Greenhouse%20Gas%20Study/GHG3%20Executive%20Summary%20and%20Report.pdf.

[33] D. Sparreboom and M. Leslie-Miller. Weather Routing of Motorsailers. In *22th International HISWA Symposium on Yacht Design and Yacht Construction*, 2012. URL http://hiswasymposium.com/assets/files/pdf/2012/Leslie-Miller.pdf.

[34] M. Stopford. Maritime Economics. Routledge, London ; New York, 3rd edition, 2009. ISBN 9780415275576 0415275571 9780415275583 (pbk.) 041527558X (pbk.) 9780203891742 (e-book) 0203891740 (e-book). URL http://www.loc.gov/catdir/toc/ecip0812/2008009223.html.

[35] A. Thom. Effect of Discs on the Air Forces on a Rotating Cylinder. Report, Aeronautical Research Committee, 1934.

[36] N.J. van der Kolk, J.A. Keuning, and R.H.M. Huijsmans. Bilge Keels for Course Stability and Sailing Efficiency of Wind-Assisted Ships. Report, Delft University of Technology, 2019. URL https://www.researchgate.net/publication/331979320_Bilge_Keels_for_Course_Stability_and_Sailing_Efficiency_of_Wind-Assisted_Ships.

[37] J. Väinämö. Operational Experiences and Results from the First Reference Installation from Nov-2014, Roro-Ship Estraden (9700 Dwt). In *24th International HISWA Symposium on Yacht Design and Yacht Construction*, 2016. URL http://www.hiswasymposium.com/wp-content/uploads/2017/06/S4-1-OPERATIONAL-EXPERIENCES-AND-RESULTS-FROM-....pdf.

[38] L.F. Whicker and L.F. Fehlner. Free-Stream Characteristics of a Family of Low-Aspect-Ratio, All-Movable Control Surfaces for Application to Ship Design. Report, DTMB, 1958.

Appendix: Case study operational characteristics

Figures hidden for confidentiality reasons.

Figure A.1: Heel angle, occurrence over all simulated voyages for both Flettner rotor (FR) configurations

Figure A.2: Yaw angle, occurrence over all simulated voyages for both Flettner rotor (FR) configurations

Figure A.3: Rudder angle, occurrence over all simulated voyages for both Flettner rotor (FR) configurations